Rolling Bodies with Regular Surface: Controllability Theory and Applications

Alessia Marigo and Antonio Bicchi, *Senior Member, IEEE*

***Abstract*—Pairs of bodies with regular rigid surfaces rolling onto each other in space form a nonholonomic system of a rather general type, posing several interesting control problems of which not much is known. The nonholonomy of such systems can be exploited in practical devices, which is very useful in robotic applications. In order to achieve all potential benefits, a deeper understanding of these types of systems and more practical algorithms for planning and controlling their motions are necessary. In this paper, we study the controllability aspect of this problem, giving a complete description of the reachable manifold for general pairs of bodies, and a constructive controllability algorithm for planning rolling motions for dexterous robot hands.**

***Index Terms*—Nonholonomic systems, nonlinear controllability theory, robotic manipulation.**

I. INTRODUCTION

NON-HOLONOMIC systems have been attracting much attention in control literature recently, due to both their relevance to practical applications (to Robotics in particular), and to the challenges involved in their planning and control [1] and [2].

Let us recall a few classical definitions from rational mechanics. Consider a mechanical system whose configurations $\boldsymbol{q}$ evolve in a smooth n-dimensional manifold $\mathcal{M}$, and whose velocities $\dot{\boldsymbol{q}} \in T_{\boldsymbol{q}}\mathcal{M}$ are subject to m locally independent constraints in the Pfaffian form

$$\boldsymbol{A}(\boldsymbol{q})\dot{\boldsymbol{q}} = 0 \tag{1}$$

where $\boldsymbol{A}$ is an $m \times n$, $m < n$ matrix of real-valued analytic functions. Constraints are said to be *holonomic* if their differential form (1) is integrable. In this case, there exists a family of integral submanifolds $\mathcal{M}' \subset \mathcal{M}$ of dimension $n - m$ that are invariant.

If the constraints are not holonomic at some $\boldsymbol{q}$, then there will exist an integral submanifold through $\boldsymbol{q}$ of dimension $n - m + k$, $0 < k \leq m$. The number k is referred to as degree of nonholonomy. If $k = m$, the constraints, and by extension the system, are said to be maximally nonholonomic.

According to the viewpoint expressed by this definition, nonholonomy is a property pertinent to constraints imposed on a system, and is usually regarded as an annoying accident inhibiting simplicity in steering and control. This is in the attitude of most drivers toward the nonholonomy of the automobile kinematics when a parallel parking maneuver is necessary.

In this paper, we take a different perspective. A convenient "control" form describing the constrained system can easily be obtained from the differential constraints (1). In fact, if we let $\boldsymbol{G}(\boldsymbol{q})$ denote a $n \times (n - m)$ matrix whose columns $\boldsymbol{g}_i(\boldsymbol{q})$, $i = 1, \cdots, n - m$ form a basis for the annihilating distribution of $\boldsymbol{A}(\boldsymbol{q})$, then all admissible velocities $\dot{\boldsymbol{q}} \in \boldsymbol{A}(\boldsymbol{q})^{\perp} \subset \boldsymbol{T_q}\mathcal{M}$ can be written as linear combinations of the columns of $\boldsymbol{G}(\boldsymbol{q})$,

$$\dot{\boldsymbol{q}} = \boldsymbol{G}(\boldsymbol{q})\boldsymbol{w} = \sum_{i=1}^{n-m} \boldsymbol{g}_i(\boldsymbol{q})\boldsymbol{w}_i \tag{2}$$

where $\boldsymbol{w}$ is a vector of *quasivelocities* taking values in $\mathbb{R}^{n-m}$. When quasivelocities can be assigned values at will in time, functions $\boldsymbol{w}$: $\mathbb{R}^{+} \rightarrow \mathbb{R}^{n-m}$, $t \mapsto \boldsymbol{w}(t)$ can be regarded as *control* inputs of the driftless, linear-in-control, nonlinear system (2). A physical *actuator* is associated to each control input $\boldsymbol{w}_i$, e.g. a motor for electromechanical systems. Nonholonomy of the original system, i.e. nonintegrability of (1), is reflected through Frobenius' theorem in the fact that the distribution $\mathrm{span}\{\boldsymbol{g}_1(\boldsymbol{q}) \cdots \boldsymbol{g}_{n-m}(\boldsymbol{q})\}$ in (2) is not involutive. In fact, let the smallest involutive distribution Δ which contains the columns of $\boldsymbol{G}(\boldsymbol{q})$ have dimension d: if $d > n - m$ the system is nonholonomic; if $d = n$, the system is maximally nonholonomic. Hence, it can be steered through any two configurations of its n-dimensional manifold along the flows of $n - m$ vector fields. Observe that the whole manifold $\mathcal{M}$ is an equilibrium manifold for the system with $\boldsymbol{w} = 0$. Controllability to an equilibrium manifold of higher dimension than the control space is not possible for any linear system, and is in fact a peculiarity of nonholonomic systems.

From an utilitarian engineer's viewpoint, the latter definition may be rephrased as "an n-dimensional nonholonomic system can be steered at will using less than n actuators." This formulation underscores the appealing fact that devices with reduced hardware complexity can be used to perform nontrivial tasks, if nonholonomy is introduced on purpose, and cleverly exploited, in the device design. Examples of systems designed according to such a philosophy have been reported by Brockett [3], Arai and Tachi [33] Sordalen and Nakamura [66]Ostrowski and Burdick [5], Nakamura and Mukherjee [4], Bicchi and Sorrentino [7].

Nonholonomy of rolling is particularly relevant to robotic manipulation, one of the main goals of which is to manipulate an object grasped by a robot end-effector so as to relocate and re-

Manuscript received January 22,1999; revised September 1999. Recommended by Associate Editor, O. Egeland. This work was conducted with partial support of NATO CR Grant 960750 and ASI ARS-96-170.

A. Marigo is with the Int. School for Advanced Studies (SISSA-ISAS), Trieste, Italy, and also with the Interdept. Research Center "Enrico Piaggio," University of Pisa, 56100 Pisa, Italy (e-mail: marigo@piaggio.ccii.unipi.it).

A. Bicchi is with the Department of Electrical Systems and Automation, University of Pisa, Italy, and also with the Interdept. Research Center "Enrico Piaggio," University of Pisa, 56100 Pisa, Italy (e-mail: bicchi@ing.unipi.it).

Publisher Item Identifier S 0018-9286(00)07500-0.

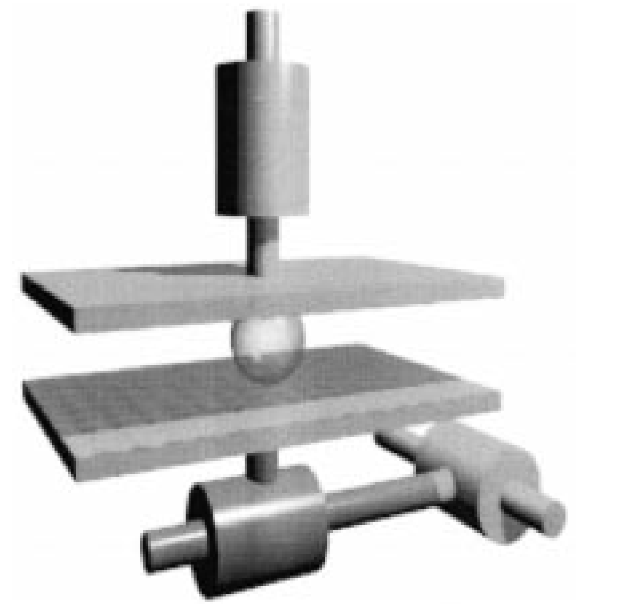

Fig. 1. The first dexterous gripper (DxGrip-I), designed at Centro "E. Piaggio," University of Pisa. The gripper has two planar parallel jaws: the upper applies a suitable grasping force on the object, while the lower translates in the plane imposing a desired rolling motion to the object. Arbitrary configurations of the object in contact with the plates can be achieved by rolling: full dexterity is obtained by adding a vertical translation of the whole gripper, by an actuator not shown in the picture.

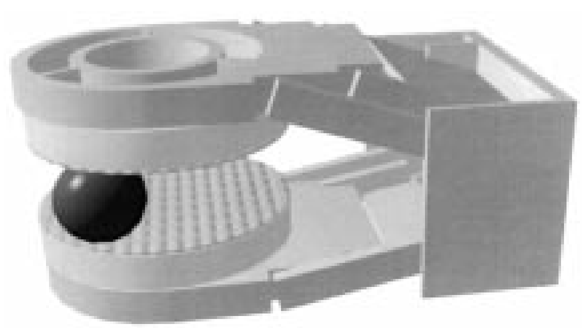

Fig. 2. The second generation dexterous gripper (DxGrip-II). The gripper has two parallel jaws translating independently, and two turning disks with direct-drive motors on each jaw, endowed also with force/torque, tactile sensors. The hand can arbitrarily relocate and reorient any convex body with regular surface by rolling it among the fingers. The design represents an industry-oriented version of DxGrip-I.

orient it arbitrarily, the so-called *dexterity* property. Dexterous robotic hands developed so far according to an anthropomorphic paradigm employ far too many joints and actuators (a minimum of nine) to be a viable industrial solution. Nonholonomy of rolling can be used to alleviate this limitation. In fact, while rolling between the surfaces of the manipulated object and that of fingers has been previously regarded as a complication to be neglected, or compensated for, work of Cole *et al.* [8] and Bicchi *et al.* [7] tried to exploit rolling for achieving dexterity with simpler mechanical hardware.

In particular, several prototype dexterous grippers have been developed at Centro "E. Piaggio" of University of Pisa, using as few as 4 actuators (see Figs. 1 and 2).

These grippers are able to perform manipulation of grasped objects by rolling them in between their fingers, and have been demonstrated with a fairly wide variety of objects and tasks. These grippers were dubbed "dexterous" based on what was actually a "generic controllability" conjecture ([7]):

Conjecture. A pair of bodies can be brought from any initial to any final relative configuration by rolling in contact with each other, except at most for nongeneric pairs.

In this paper, we prove the above conjecture, characterize precisely what pairs of surfaces are not controllable, and describe the structure of the reachable manifolds in all cases. Furthermore, we consider the constructive controllability problem, and provide an algorithm to steer a system of rolling bodies through two arbitrary reachable configurations.

A. Related Work

Introducing nonholonomy on purpose in the design of robotic mechanisms can be regarded as a means of lifting complexity from hardware to the software and control level of design. In fact, planning and controlling nonholonomic systems is in general a considerably more difficult task than for holonomic systems. The very fact that there are fewer degrees-of-freedom available than there are configurations implies that standard motion planning techniques can not be directly adapted to nonholonomic systems. From the control viewpoint, nonholonomic systems are intrinsically nonlinear systems, in the sense that they are not exactly feedback linearizable, nor does their linear approximation retain the fundamental characteristics of the system, such as controllability. Simple, continuous, time-invariant feedback control laws, on the other hand, can not be applied to stabilizing nonholonomic, nonsingular systems [9].

An important class of nonholonomic systems for which a reasonably satisfactory understanding has recently been reached is the class of two-input nilpotentizable systems that can be put, by feedback transformation, in the so-called "chained" form. A complete characterization of such systems (i.e., necessary and sufficient conditions for the existence of a feedback transformation to chained-form) has been provided by Murray [10], while an algorithm for finding the necessary coordinate transform has been presented by Tilbury, Murray, and Sastry [11]. For example, a car pulling an arbitrary number of trailers has been shown to be a chained-form system by Sordalen [12]. Planning algorithms for chained-form systems in free space have been described by several authors: in his early work, Brockett [13] used sinusoidal inputs, which were subsequently investigated in more detail by Murray and Sastry [14]. The methods of Lafferriere and Sussmann [15], Monaco and Normand-Cyrot [16], and Jacobs [17], using piecewise constant inputs in different arrangements, are particularly well-suited to chained systems, where they achieve exact planning. Only approximate, iterative planning schemes are obtained in the general case. Furthermore, chained systems are *differentially flat*, and therefore the techniques of Rouchon *et al.* [18] can be profitably applied.

Unfortunately, the system of rolling bodies considered in this paper differs substantially from the class of chained form systems. Consider, for example, the case such of the *plate-ball* system, which is a classical problem in rational mechanics, brought to the attention of the control community by Brockett and Dai [13]. The plate-ball system is a 5-dimensional, 2-input nonholonomic system, which is not differentially flat [19], and can be regarded as an instance of the famous 5-variables problem of Cartan. Montana [20] derived a differential-geometric model of the rolling constraint between general bodies, and discussed applications to robotic manipulation. Li and Canny [21] showed that the plate-ball system is controllable, and that the same holds for two rolling spheres, provided that their radius is different. Jurdjevic [22] studied the problem of finding the path that minimizes the length of the curve traced out by the sphere on the fixed plane. It turns out that optimal paths also minimize the integral of their geodesic curvature, so that solutions are those of Euler's *elastica* problem. Levi [23] gave explicit formulas for evaluating the final configuration of the ball after a circular motion of the plate.

This paper is organized into four main sections. In Section II, we derive a complete mathematical model of rolling between arbitrary surfaces. Section III explains our main theorem, concerning the proof of the conjecture above and the study of the structure of the reachable manifold for a system of rolling bodies. Finally in Section IV, we describe a planning algorithm for manipulating an object of arbitrary shape by rolling between two plates.

II. Kinematic Model of Rolling Bodies

In this section, we report the derivation of a mathematical model of rolling between regular geometric surfaces (II-A), and on the restrictions imposed by the impenetrability of rigid bodies on admissible contacts (II-B). The kinematic model obtained in II-A is not completely new in the literature when compared with [20], [24], but is derived here in a different way, which is useful to report for the rest of our development (specifically, breaking up Montana's equations in (12) and (18), allows the analysis of admissibility of rolling reported in Section II-B-2).

A. Kinematics of Rolling Surfaces

Consider two arbitrary regular surfaces S_1, S_2 in touch at a point $\boldsymbol{c}$ as represented in Fig. 3. Let the two surfaces be described, in a neighborhood of the contact point, by two orthogonal parameterizations as

$$\boldsymbol{f}\colon \mathbb{R}^2 \longrightarrow \mathbb{R}^3,\ \boldsymbol{f}(u, v) = (f_1(u, v),\ f_2(u, v),\ f_3(u, v))$$
$$\boldsymbol{h}\colon \mathbb{R}^2 \longrightarrow \mathbb{R}^3,\ \boldsymbol{h}(x, y) = (h_1(x, y),\ h_2(x, y),\ h_3(x, y))$$

respectively. These parameterizations induce Gauss frames $\mathcal{G}_1(u, v)$ and $\mathcal{G}_2(x, y)$, defined at every point in the contact neighborhood with axes $\hat{\boldsymbol{f}}_u = (\boldsymbol{f}_u^T/\|\boldsymbol{f}_u\|)$, $\hat{\boldsymbol{f}}_v = (\boldsymbol{f}_v^T/\|\boldsymbol{f}_v\|)$, $\boldsymbol{n}_1 = (\boldsymbol{f}_u \wedge \boldsymbol{f}_v/\|\boldsymbol{f}_u\|\|\boldsymbol{f}_v\|)$ and $\hat{\boldsymbol{h}}_x = (\boldsymbol{h}_x^T/\|\boldsymbol{h}_x\|)$, $\hat{\boldsymbol{h}}_y = (\boldsymbol{h}_y^T/\|\boldsymbol{h}_y\|)$, $\boldsymbol{n}_2 = (\boldsymbol{h}_x \wedge \boldsymbol{h}_y/\|\boldsymbol{h}_x\|\|\boldsymbol{h}_y\|)$, respectively We will use here and henceforth the shorthand notation $\boldsymbol{f}_u = (\partial \boldsymbol{f}/\partial u)$, etc.

To take the rigid-body motions of our surfaces into account, we introduce time dependencies of the geometric quantities introduced above by defining new maps $\mathcal{G}_i'\colon \mathbb{R}^2 \times \mathbb{R} \rightarrow SE(3) \times \mathbb{R}$, $i = 1, 2$ as $\mathcal{G}_i' = g_i(t) \circ \mathcal{G}_i$, with $g_i(t) = (\boldsymbol{R}_i, \boldsymbol{p}_i) \in SE(3)$. By a slight abuse of notation, we will indicate that $\boldsymbol{f}(u, v, t) = g_1(t) \circ \boldsymbol{f}(u, v)$, and $\boldsymbol{h}(x, y, t) = g_2(t) \circ \boldsymbol{h}(x, y)$. We also introduce the notation $\boldsymbol{\eta} = (\boldsymbol{t}, \boldsymbol{\omega}) \in se(3)$ for the elements of the tangent space of $SE(3)$.

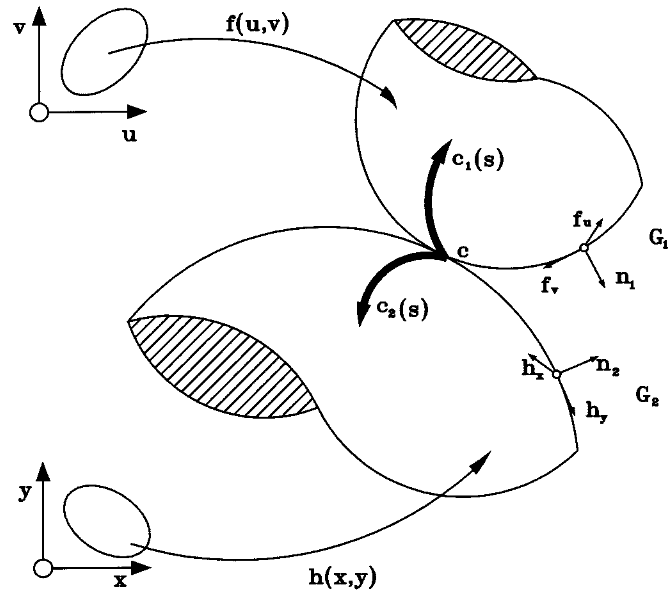

Fig. 3. A pair of smooth rolling surfaces.

At the contact point, $\boldsymbol{n}_2 = -\boldsymbol{n}_1$, while the first axes of the two Gauss frames form an angle

$$\psi = -\arccos \hat{\boldsymbol{f}}_u^T \hat{\boldsymbol{h}}_x. \tag{3}$$

We locally describe the configuration space of the system as the 5-dimensional manifold $\mathcal{M}$ with coordinates $\boldsymbol{q} = [u \quad v \quad x \quad y \quad \psi]^T$. This choice of parameterization directly eliminates the obviously holonomic constraint of zero penetration-detachment velocity between the two surfaces.

Let two smooth directed curves on the surfaces be $\boldsymbol{c}_1 = \boldsymbol{f}(u(s_1), v(s_1), t)$, $\boldsymbol{c}_2 = \boldsymbol{h}(x(s_2), y(s_2), t)$ (see Fig. 3), and let the two curves be parametrized by the arc lengths s_1, s_2, respectively. Consider the family of rigid motions of S_1 relative to S_2, the latter assumed fixed in space, such that the contact point traces out the curves on the two surfaces in the given directions at different velocities. Rolling without slipping between the two surfaces imposes the constraint that the length of the paths covered by the image of the contact point on the two curves in a corresponding time are equal, $s_1(t) \equiv s_2(t) \stackrel{def}{=} s(t)$. Furthermore, points of the surfaces which are in contact at the time of concern have zero relative velocity,

$$\dot{\boldsymbol{c}}_1 = \frac{\partial \boldsymbol{c}_1}{\partial t} + \frac{\partial \boldsymbol{c}_1}{\partial s}\dot{s} = \dot{\boldsymbol{c}}_2 = \frac{\partial \boldsymbol{c}_2}{\partial t} + \frac{\partial \boldsymbol{c}_2}{\partial s}\dot{s}. \tag{4}$$

This equation must hold in particular for $\dot{s} = 0$, and from the assumption $g_2(t) \equiv Id$ it easily follows that the translational velocity of S_1, $\boldsymbol{t}_1(t) = (\partial \boldsymbol{f}(u, v, t)/\partial t)$, must be zero, hence $(\partial \boldsymbol{c}_1/\partial t) = (\partial \boldsymbol{c}_2/\partial t) = 0$. From (4) one gets

$$\frac{\partial \boldsymbol{c}_1}{\partial s} = (\boldsymbol{f}_u u_s + \boldsymbol{f}_v v_s) = \frac{\partial \boldsymbol{c}_2}{\partial s} = (\boldsymbol{h}_x x_s + \boldsymbol{h}_y y_s). \tag{5}$$

Multiplying both sides of (5) by $\boldsymbol{f}_u^T$ one has

$$\begin{aligned}\|\boldsymbol{f}_u\|^2 u_s &= \boldsymbol{f}_u^T \boldsymbol{h}_x x_s + \boldsymbol{f}_u^T \boldsymbol{h}_y y_s \\ &= \|\boldsymbol{f}_u\|\,\|\boldsymbol{h}_x\|\,\cos(\psi) x_s - \|\boldsymbol{f}_u\|\,\|\boldsymbol{h}_y\|\,\sin(\psi) y_s\end{aligned}$$

while, multiplying by $\boldsymbol{f}_v^T$,

$$\|\boldsymbol{f}_v\|^2 v_s = -\|\boldsymbol{f}_v\| \|\boldsymbol{h}_x\| \sin(\psi) x_s - \|\boldsymbol{f}_v\| \|\boldsymbol{h}_y\| \cos(\psi) y_s.$$

Dividing the results by $\|\boldsymbol{f}_u\|$ and $\|\boldsymbol{f}_v\|$, respectively, and by letting $\boldsymbol{M}_1 = \operatorname{diag}(\|\boldsymbol{f}_u\|, \|\boldsymbol{f}_v\|)$, $\boldsymbol{M}_2 = \operatorname{diag}(\|\boldsymbol{h}_x\|, \|\boldsymbol{h}_y\|)$, these equations can be rewritten more compactly as

$$\boldsymbol{M}_1 \begin{bmatrix} u_s \\ v_s \end{bmatrix} - \boldsymbol{R}_\psi \boldsymbol{M}_2 \begin{bmatrix} x_s \\ y_s \end{bmatrix} = 0 \tag{6}$$

where matrix

$$\boldsymbol{R}_\psi = \begin{bmatrix} \cos(\psi) & -\sin(\psi) \\ -\sin(\psi) & -\cos(\psi) \end{bmatrix}$$

takes into account the relative orientation of the axes of the Gauss frames on the tangent plane. Notice that $\boldsymbol{R}_\psi = \boldsymbol{R}_\psi^{-1}$. Also observe that matrices $\boldsymbol{M}_i$ are the symmetric, positive definite square roots of the first fundamental form of the surfaces, i.e. $\boldsymbol{M}_i^T \boldsymbol{M}_i = \mathcal{I}_i$, i.e., the Riemannian metric forms of the ith surface. The Pfaffian form of the rolling-without-sliding constraint (6) is therefore

$$[\boldsymbol{M}_1 \quad -\boldsymbol{R}_\psi \boldsymbol{M}_2 \quad 0]\, \dot{\boldsymbol{q}} = 0. \tag{7}$$

It should be noticed that a "spinning" rotation of the two bodies about the common normal direction is still allowed if only constraint (6) is enforced. This type of "spinning" motion is actually difficult to actuate in most practical cases of manipulation, and very often friction and micro-deformations near the contact point constrain spinning velocity to be zero. Therefore, in these cases a further constraint is to be considered in which the relative angular velocity $\boldsymbol{\omega}$ has zero component along the common normal direction at the contact point, that

$$\boldsymbol{n}^T \boldsymbol{\omega} = \frac{\partial \psi}{\partial t} = 0. \tag{8}$$

As the contact points move on $\boldsymbol{c}_1(s)$, $\boldsymbol{c}_2(s)$, by derivation of (3), noticing that, for any unit vector $\boldsymbol{z}$, $((d/ds)\boldsymbol{z})^T \boldsymbol{z} = 0$, and using the facts

$$\begin{aligned} \hat{\boldsymbol{h}}_x &= \hat{\boldsymbol{f}}_u \cos\psi - \hat{\boldsymbol{f}}_v \sin\psi \\ \hat{\boldsymbol{f}}_u &= \hat{\boldsymbol{h}}_x \cos\psi - \hat{\boldsymbol{h}}_y \sin\psi \end{aligned} \tag{9}$$

one gets

$$\dot{\psi} = \frac{\partial \psi}{\partial s}\dot{s} + \frac{\partial \psi}{\partial t} = \left(\left(\frac{d}{ds}\hat{\boldsymbol{f}}_u \right)^T \left(\hat{\boldsymbol{f}}_v \right) + \left(\frac{d}{ds}\hat{\boldsymbol{h}}_x \right)^T \left(\hat{\boldsymbol{h}}_y \right) \right) \dot{s}. \tag{10}$$

Expanding the derivatives and introducing Cartan's notation of *torsion forms*

$$\boldsymbol{T}_1 = \left[\frac{\boldsymbol{f}_v^T \boldsymbol{f}_{uu}}{\|\boldsymbol{f}_u\|^2 \|\boldsymbol{f}_v\|} \; \frac{\boldsymbol{f}_v^T \boldsymbol{f}_{uv}}{\|\boldsymbol{f}_u\| \|\boldsymbol{f}_v\|^2} \right]$$

and

$$\boldsymbol{T}_2 = \left[\frac{\boldsymbol{h}_y^T \boldsymbol{h}_{xx}}{\|\boldsymbol{h}_x\|^2 \|\boldsymbol{h}_y\|} \; \frac{\boldsymbol{h}_y^T \boldsymbol{h}_{xy}}{\|\boldsymbol{h}_x\| \|\boldsymbol{h}_y\|^2} \right]$$

the constraint of rolling without spinning (10) can be rewritten, together with constraint (6), in Pfaffian form as

$$\begin{bmatrix} \boldsymbol{M}_1 & -\boldsymbol{R}_\psi \boldsymbol{M}_2 & 0 \\ \boldsymbol{T}_1 \boldsymbol{M}_1 & \boldsymbol{T}_2 \boldsymbol{M}_2 & -1 \end{bmatrix} \dot{\boldsymbol{q}} = 0. \tag{11}$$

Rolling motions subject to (11) will be called "pure" rolling motions.

The control form of the kinematic model of rolling bodies under constraint of no sliding is obtained by calculating the annihilating distribution of the constraint (7) as

$$\dot{\boldsymbol{q}} = \begin{bmatrix} \boldsymbol{M}_1^{-1} & 0 \\ \boldsymbol{M}_2^{-1} \boldsymbol{R}_\psi & 0 \\ 0 & 1 \end{bmatrix} \begin{bmatrix} w_1 \\ w_2 \\ w_3 \end{bmatrix} \tag{12}$$

while for pure rolling, by annihilating (11) one has

$$\dot{\boldsymbol{q}} = \boldsymbol{G}(\boldsymbol{q}) \boldsymbol{w} = \begin{bmatrix} \boldsymbol{M}_1^{-1} \\ \boldsymbol{M}_2^{-1} \boldsymbol{R}_\psi \\ \boldsymbol{T}_1 + \boldsymbol{T}_2 \boldsymbol{R}_\psi \end{bmatrix} \begin{bmatrix} w_1 \\ w_2 \end{bmatrix}. \tag{13}$$

The relationship of the pseudo-velocity inputs $\boldsymbol{w}$ to the physically accessible variables, i.e. to the relative angular velocity of the bodies $\boldsymbol{\omega}$, can be calculated as follows. For a unit vector $\boldsymbol{z}$ fixed on a rigid body moving with $\boldsymbol{\eta} = (0, \boldsymbol{\omega}) \in se(3)$, it holds $\dot{\boldsymbol{z}} = \boldsymbol{\omega} \wedge \boldsymbol{z}$. Solving for $\boldsymbol{\omega}$ one gets $\boldsymbol{\omega} = \boldsymbol{z} \wedge \dot{\boldsymbol{z}} + \lambda \boldsymbol{z}$, with $\lambda \in \mathbb{R}$ undetermined. Applying this formula to vectors $\boldsymbol{n}_1$, $\hat{\boldsymbol{f}}_u$ fixed on S_1, and $\boldsymbol{n}_2$, $\hat{\boldsymbol{h}}_x$ fixed on S_2, and expressing the motion of the bodies with respect to an observer fixed on the moving tangent plane at the contact point, one gets the relationships

$$\begin{aligned} \boldsymbol{\omega}_1 &= \boldsymbol{n}_1 \wedge \dot{\boldsymbol{n}}_1 + \lambda_1 \boldsymbol{n}_1 && (14) \\ &= \hat{\boldsymbol{f}}_u \wedge \dot{\hat{\boldsymbol{f}}}_u + \gamma_1 \hat{\boldsymbol{f}}_u && (15) \\ \boldsymbol{\omega}_2 &= \boldsymbol{n}_2 \wedge \dot{\boldsymbol{n}}_2 + \lambda_2 \boldsymbol{n}_2 && (16) \\ &= \hat{\boldsymbol{h}}_x \wedge \dot{\hat{\boldsymbol{h}}}_x + \gamma_2 \hat{\boldsymbol{h}}_x. && (17) \end{aligned}$$

The components of $\boldsymbol{\omega}_1$ and $\boldsymbol{\omega}_2$ along the axes of the Gauss frames $\mathcal{G}_1$, $\mathcal{G}_2$, respectively, are computed using (14)–(17) as

$$\boldsymbol{\omega}_1 = \begin{bmatrix} \boldsymbol{\omega}_1^T \hat{\boldsymbol{f}}_u \\ \boldsymbol{\omega}_1^T \hat{\boldsymbol{f}}_v \\ \boldsymbol{\omega}_1^T \boldsymbol{n}_1 \end{bmatrix} = \begin{bmatrix} -\hat{\boldsymbol{f}}_v^T \dot{\boldsymbol{n}}_1 \\ \hat{\boldsymbol{f}}_u^T \dot{\boldsymbol{n}}_1 \\ \hat{\boldsymbol{f}}_v^T \dot{\hat{\boldsymbol{f}}}_u \end{bmatrix}$$

$$\boldsymbol{\omega}_2 = \begin{bmatrix} \boldsymbol{\omega}_2^T \hat{\boldsymbol{h}}_x \\ \boldsymbol{\omega}_2^T \hat{\boldsymbol{h}}_y \\ \boldsymbol{\omega}_2^T \boldsymbol{n}_2 \end{bmatrix} = \begin{bmatrix} -\hat{\boldsymbol{h}}_y^T \dot{\boldsymbol{n}}_2 \\ \hat{\boldsymbol{h}}_u^T \dot{\boldsymbol{n}}_2 \\ \hat{\boldsymbol{h}}_y^T \dot{\hat{\boldsymbol{h}}}_x \end{bmatrix}.$$

The relative angular velocity expressed in $\mathcal{G}_1$ is

$$\boldsymbol{\omega} = \boldsymbol{\omega}_1 + \left[\begin{array}{c|c} \boldsymbol{R}_\psi & \boldsymbol{0} \\ \hline \boldsymbol{0} & 1 \end{array} \right] \boldsymbol{\omega}_2.$$

By expanding the derivatives of $\boldsymbol{n}_1$, $\boldsymbol{n}_2$, $\hat{\boldsymbol{f}}_u$ and $\hat{\boldsymbol{h}}_x$ and comparing with equation (12), one gets

$$\boldsymbol{\omega} = \boldsymbol{S} \left[\begin{array}{c|c} -\boldsymbol{M}_1^{-1} \mathcal{II}_1 \boldsymbol{M}_1^{-1} - \boldsymbol{R}_\psi \boldsymbol{M}_2^{-1} \mathcal{II}_2 \boldsymbol{M}_2^{-1} \boldsymbol{R}_\psi & 0 \\ \hline -\boldsymbol{T}_1 - \boldsymbol{T}_2 \boldsymbol{R}_\psi & 1 \end{array} \right] \boldsymbol{w}$$

where $\mathcal{II}_i$ is the second fundamental form of surface S_i, and

$$\boldsymbol{S} = \begin{bmatrix} 0 & 1 & 0 \\ -1 & 0 & 0 \\ 0 & 0 & 1 \end{bmatrix}.$$

Observing that

$$-\boldsymbol{M}_1^{-1}\mathcal{II}_1\boldsymbol{M}_1^{-1} = \begin{bmatrix} \dfrac{\boldsymbol{f}_u^T\boldsymbol{n}_{1u}}{\|\boldsymbol{f}_u\|^2} & \dfrac{\boldsymbol{f}_u^T\boldsymbol{n}_{1v}}{\|\boldsymbol{f}_u\|\,\|\boldsymbol{f}_v\|} \\ \dfrac{\boldsymbol{f}_v^T\boldsymbol{n}_{1u}}{\|\boldsymbol{f}_u\|\,\|\boldsymbol{f}_v\|} & \dfrac{\boldsymbol{f}_v^T\boldsymbol{n}_{1v}}{\|\boldsymbol{f}_v\|^2} \end{bmatrix} = \boldsymbol{K}_1$$

$$-\boldsymbol{M}_2^{-1}\mathcal{II}_2\boldsymbol{M}_2^{-1} = \begin{bmatrix} \dfrac{\boldsymbol{h}_x^T\boldsymbol{n}_{2x}}{\|\boldsymbol{h}_x\|^2} & \dfrac{\boldsymbol{h}_x^T\boldsymbol{n}_{2y}}{\|\boldsymbol{h}_x\|\,\|\boldsymbol{h}_y\|} \\ \dfrac{\boldsymbol{h}_y^T\boldsymbol{n}_{2x}}{\|\boldsymbol{h}_x\|\,\|\boldsymbol{h}_y\|} & \dfrac{\boldsymbol{h}_y^T\boldsymbol{n}_{2y}}{\|\boldsymbol{h}_y\|^2} \end{bmatrix} = \boldsymbol{K}_2$$

where $\boldsymbol{K}_1$ and $\boldsymbol{K}_2$ are the *curvature forms* for the two surfaces, and introducing the *relative curvature form*

$$\boldsymbol{K}_R = \boldsymbol{K}_1 + \boldsymbol{R}_\psi\boldsymbol{K}_2\boldsymbol{R}_\psi$$

a more compact equation is obtained as

$$\boldsymbol{\omega} = \boldsymbol{S}\begin{bmatrix} \boldsymbol{K}_R & 0 \\ -\boldsymbol{T}_1 - \boldsymbol{T}_2\boldsymbol{R}_\psi & 1 \end{bmatrix}\begin{bmatrix} w_1 \\ w_2 \\ w_3 \end{bmatrix}. \tag{18}$$

When the no-spinning model of (11) and (13) is used, it will suffice to set $w_3 = 0$ in (18) [see (8)].

B. Admissibility of Rolling Contacts

Rolling contacts of impenetrable solid objects imposes some additional constraints than those studied in the previous section for geometric surfaces. We will model henceforth objects as closed subsets of $\mathbb{R}^3$, whose boundary is a surface on which the normal direction is conventionally taken to be directed outward. In the sequel, we will deal with conditions for admissibility of contact *per se*, and of rolling motions, separately.

1) Contact Admissibility:

Definition 1: A contact is locally admissible if the intersection of the interior parts of the objects in a neighborhood B_c of the contact point $\boldsymbol{f}(\overline{u}, \overline{v}) = \boldsymbol{h}(\overline{x}, \overline{y})$ is void.

Simple conditions for admissibility of contact can be stated as follows:

Lemma 1: If the contact between two surfaces at a point $\boldsymbol{f}(\overline{u}, \overline{v}) = \boldsymbol{h}(\overline{x}, \overline{y})$, with relative orientation ψ, is locally admissible, then the relative curvature form $\boldsymbol{K}_R$ is nonnegative definite. If $\boldsymbol{K}_R$ is positive definite, then the contact is locally admissible.

Proof: Local admissibility is equivalent to the following statement: for any two points $\boldsymbol{f}(u, v)$, $\boldsymbol{h}(x, y)$ on $S_1 \cap B_c$ and $S_2 \cap B_c$ for which the vector $\boldsymbol{f}(u, v) - \boldsymbol{h}(x, y)$ is parallel to the contact normal, it holds

$$(\boldsymbol{f}(u, v) - \boldsymbol{h}(x, y))^T\boldsymbol{n}_1 = \boldsymbol{n}_1^T\boldsymbol{f}(u, v) + \boldsymbol{n}_2^T\boldsymbol{h}(x, y) \le 0. \tag{19}$$

Considering the second-order development of $\boldsymbol{f}(u, v)$ about the point of contact, the signed distance to the tangent plane is given by

$$\begin{aligned}\boldsymbol{n}_1^T\boldsymbol{f}(u, v) &\approx \boldsymbol{n}_1^T\boldsymbol{f}(\overline{u}, \overline{v}) + \tfrac{1}{2}\left[\boldsymbol{n}_{1u}^T\boldsymbol{f}_u(\delta u)^2 + \boldsymbol{n}_{1u}^T\boldsymbol{f}_v(\delta u)(\delta v)\right.\\ &\quad \left. + \boldsymbol{n}_{1v}^T\boldsymbol{f}_u(\delta u)(\delta v) + \boldsymbol{n}_{1v}^T\boldsymbol{f}_v(\delta v)^2\right],\\ &= \boldsymbol{n}_1^T\boldsymbol{f}(\overline{u}, \overline{v}) - \tfrac{1}{2}[\delta u \quad \delta v]\boldsymbol{M}_1\boldsymbol{K}_1\boldsymbol{M}_1\begin{bmatrix}\delta u \\ \delta v\end{bmatrix}\end{aligned}$$

where $\delta u = (u - \overline{u})$ and $\delta v = (v - \overline{v})$, and the relation of orthogonality between $\boldsymbol{n}_1$, $\hat{\boldsymbol{f}}_u$ and $\hat{\boldsymbol{f}}_v$ have been used. Similarly we obtain the expression for the second surface as

$$\boldsymbol{n}_2^T\boldsymbol{h}(x, y) \approx \boldsymbol{n}_2^T\boldsymbol{h}(\overline{x}, \overline{y}) - \tfrac{1}{2}[\delta x \quad \delta y]\boldsymbol{M}_2\boldsymbol{K}_2\boldsymbol{M}_2\begin{bmatrix}\delta x \\ \delta y\end{bmatrix}.$$

Points $\boldsymbol{f}(u, v)$, $\boldsymbol{h}(x, y)$ such that $\boldsymbol{f}(u, v) - \boldsymbol{h}(x, y)$ is parallel to $\boldsymbol{n}_1$ share the same projection ζ, ξ on the tangent plane. Their coordinates relative to the contact point can hence be evaluated as

$$\begin{bmatrix}\delta u \\ \delta v\end{bmatrix} = \boldsymbol{M}_1^{-1}\begin{bmatrix}\delta\zeta \\ \delta\xi\end{bmatrix}; \quad \begin{bmatrix}\delta x \\ \delta y\end{bmatrix} = \boldsymbol{M}_2^{-1}\boldsymbol{R}_\psi\begin{bmatrix}\delta\zeta \\ \delta\xi\end{bmatrix}.$$

Hence we obtain

$$\begin{aligned}&\boldsymbol{n}_2^T\boldsymbol{h}(x, y)\\ &\quad \approx \boldsymbol{n}_2^T\boldsymbol{h}(\overline{x}, \overline{y}) - \tfrac{1}{2}[\delta u \quad \delta v]\boldsymbol{M}_1^T\boldsymbol{R}_\psi\boldsymbol{K}_2\boldsymbol{R}_\psi\boldsymbol{M}_1\begin{bmatrix}\delta u \\ \delta v\end{bmatrix}.\end{aligned}$$

The contact admissibility condition (19) in a neighborhood of the contact point can therefore be written

$$\tfrac{1}{2}[\delta u \quad \delta v]\boldsymbol{M}_1\boldsymbol{K}_R\boldsymbol{M}_1\begin{bmatrix}\delta u \\ \delta v\end{bmatrix} \ge 0.$$

The necessity that $\boldsymbol{K}_R$ is nonnegative definite follows directly. If $\boldsymbol{K}_R$ is positive definite, on the other hand, then there exists some a neighborhood B_c where contact is admissible, which proves the sufficiency claim. Furthermore, the contact point is isolated in that neighborhood. A pair of surfaces in a configuration with $\boldsymbol{K}_R$ positive definite is called *relatively strictly convex*. If $\mathtt{rank}(\boldsymbol{K}_R) = 1$ with $\boldsymbol{K}_R$ nonnegative definite, contact may not be admissible. If it is, there exists a one-dimensional manifold of contact points [the tangent bundle to this manifold being $\mathtt{ker}(\boldsymbol{K}_R)$]. A pair of surfaces in such configuration are called *relatively weakly convex*. If $\mathtt{rank}(\boldsymbol{K}_R) = 0$, contact may not be admissible. If it is, there exists a two-dimensional manifold of contact points. Such a pair of surfaces is called *relatively flat*, or conformal. Note that these concepts are strictly local. If $\boldsymbol{K}_R$ is not definite, or nonpositive definite, the contact is not admissible. ■

2) Admissibility of Rolling:

Definition 2: A rolling motion between two surfaces in an admissible contact configuration is admissible with respect to constraints (7), [resp., (11)] if there exist some nonzero relative angular velocity such that (7) [(11)] are satisfied at each point of contact. An admissible rolling motion is said to have p degrees-of-freedom, DOFs, if there exists a p-dimensional linear space of angular velocities satisfying (7) [(11)].

Lemma 2: Locally around an admissible contact configuration, the DOFs of admissible rolling motions are as reported in Table I.

The case $\texttt{rank}(\boldsymbol{K}_R) = 1$, $p = 1$ holds if and only if the contact manifold is linear.

Proof: Recall the relation (18) between the relative angular velocity $\boldsymbol{\omega}$ and the velocity along the unconstrained directions $\boldsymbol{w}$, and the fact that, under constraints (11), $w_3 = 0$. The two cases with $\texttt{rank}(\boldsymbol{K}_R) = 2$, and the case with $\texttt{rank}(\boldsymbol{K}_R) = 0$ under constraints (11) follow directly.

When the contact manifold is not an isolated point, condition (7) must hold at every point in the contact manifold. Because only one axis of fixed points may exist under a rotation $\boldsymbol{\omega}_3 = w_3$, and this axis is normal to the surfaces, w_3 must be zero to avoid slippage at some points of the contact manifold, hence condition (6) alone is equivalent to (6) and (10). The case $\texttt{rank}(\boldsymbol{K}_R) = 0$ under constraint (7) follows.

If $\texttt{rank}(\boldsymbol{K}_R) = 1$, using the fact that the left upper 2-by-2 block of $\boldsymbol{S}$ is antisymmetric, and that $\boldsymbol{K}_R = \boldsymbol{K}_R^T$, one gets

$$\begin{bmatrix} 0 & -1 \\ 1 & 0 \end{bmatrix} \begin{bmatrix} \boldsymbol{\omega}_1 \\ \boldsymbol{\omega}_2 \end{bmatrix} \in \texttt{range}\,(\boldsymbol{K}_R) \Rightarrow \begin{bmatrix} \boldsymbol{\omega}_1 \\ \boldsymbol{\omega}_2 \end{bmatrix} \in \texttt{ker}\,(\boldsymbol{K}_R). \tag{20}$$

From the fact that $\boldsymbol{\omega}$ is the same for all points of the rolling bodies, and that $\texttt{ker}(\boldsymbol{K}_R)$ is the tangent bundle to the contact manifold and is one-dimensional, it follows that the contact manifold must be a line segment. Rolling will be possible around an axis including the segment, as in the case of a cylinder or a cone rolling on a plane. ∎

Based on the two preceding lemmata, a classification of rolling pairs ensues which is reported in Appendix A.

III. Study of the Reachable Manifold

In this section we investigate the conjecture reported in the introduction, and more particularly the degree of nonholonomy of the rolling constraints (7) and (11), by analyzing the structure of the reachable manifold for the control systems (12) and (13), respectively. We will first focus our attention on the case that the pure rolling constraints (11) are enforced, i.e., on the control form of the kinematics of pure rolling (13).

Notice that in (13), inputs $\boldsymbol{w}$ may possibly be subject to restrictions entailed [because of (18)] by limitations on admissible $\boldsymbol{\omega}$ as discussed in Section II-B. For instance, for two conformal surfaces having $\texttt{rank}(\boldsymbol{K}_R) = 0$ and zero DOF.'s, (13) degenerates to the trivial equation $\dot{\boldsymbol{q}} = \boldsymbol{0}$ by imposing $\boldsymbol{w} = 0$.

A. Relatively Weakly Convex Bodies

Consider an admissible contact of a pair of relatively weakly convex bodies, which instantaneously has one rolling DOF. By equations (18) and (20), $\boldsymbol{\omega} \in \texttt{ker}(\boldsymbol{K}_R) \Rightarrow \boldsymbol{w} \in \texttt{range}(\boldsymbol{K}_R)$, hence the control form (13) has only one independent input at such configurations.

If the set of configurations for which $\texttt{rank}(\boldsymbol{K}_R) = 1$ is open in the configuration manifold $\mathcal{M}$, the control system (13) has a single nonsingular control vector field, which is obviously involutive. Therefore, the reachable submanifold is a one-dimensional submanifold of $\mathcal{M}$. An example is a cylinder (or a cone) rolling on a plane, for which the allowed angular velocity is always perpendicular to the line of contact.

TABLE I
DOFs of Admissible Rolling Motions

	Constr. (7)	Constr. (11)
rank $(\mathbf{K}_R) = 2$	$p = 3$	$p = 2$
rank $(\mathbf{K}_R) = 1$	$p \leq 1$	$p \leq 1$
rank $(\mathbf{K}_R) = 0$	$p = 0$	$p = 0$

If otherwise $\texttt{rank}(\boldsymbol{K}_R) = 1$ in a submanifold of $\mathcal{M}$ including the contact configuration $\bar{\boldsymbol{q}}$, the control system (13) has a singularity in $\bar{\boldsymbol{q}}$. Due to analyticity of the manifold and of the control equations, there will be maximal integral submanifolds for the system motion [25]. However, the dimension of these submanifolds may vary from one (as in the case of two cylinders rolling on each other with aligned axes), to five. An example of the latter extreme is provided by a cone rolling on a cylinder, starting with aligned axes: all infinitesimal rolling motions take the relative configuration out of the singularity [where $\texttt{rank}(\boldsymbol{K}_R) = 1$], and make the bodies relatively convex [$\texttt{rank}(\boldsymbol{K}_R) = 2$]. Maximal nonholonomy will follow from Theorem 1 in the next section.

B. Relatively Convex Bodies

We consider now the "genuine" 3D rolling case where the contact point is isolated, $\boldsymbol{K}_R$ is full rank, and the system has two DOF.'s. The main result of this paper is as follows:

Theorem 1: The pure rolling contact constraints (11) between two relatively strictly convex surfaces are:

a) holonomic if and only if bodies are specular images of each other;
b) maximally nonholonomic otherwise.

Remark 1: In nonlinear control terms, the thesis can be rephrased as

a) $\dim\langle \boldsymbol{g}_1(\boldsymbol{q}), \boldsymbol{g}_2(\boldsymbol{q}) | \boldsymbol{g}_1(\boldsymbol{q}), \boldsymbol{g}_2(\boldsymbol{q})\rangle = 2$ iff specular;
b) $\dim\langle \boldsymbol{g}_1(\boldsymbol{q}), \boldsymbol{g}_2(\boldsymbol{q}) | \boldsymbol{g}_1(\boldsymbol{q}), \boldsymbol{g}_2(\boldsymbol{q})\rangle = 5$ otherwise;

where $\boldsymbol{g}_1, \boldsymbol{g}_2$ denote the vector fields forming the columns of $\boldsymbol{G}(\boldsymbol{q})$ in (13), and $\langle\cdot|\cdot\rangle$ denotes the smallest distribution containing the second argument, which is invariant under Lie-bracketing with the first argument.

Roughly speaking, two bodies are said specular if they are, locally around the contact point, the mirror image of each other. A mathematical definition of specularity is given as follows. Recall that the image of a surface $\boldsymbol{h}(x, y)$ through a rigid motion $g = (\boldsymbol{R}, \boldsymbol{z}) \in SE(3)$ is defined as $g \circ \boldsymbol{h}(x, y) = \boldsymbol{R}\boldsymbol{h}(x, y) + \boldsymbol{z}$. Let $s = (\hat{\boldsymbol{\Sigma}}, \hat{\boldsymbol{t}})$, with $\hat{\boldsymbol{\Sigma}} \in O(3)$ and $\det(\hat{\boldsymbol{\Sigma}}) = -1$, and $\hat{\boldsymbol{t}} \in \mathbb{R}^3$ denote a symmetry. In particular, by taking $\hat{\boldsymbol{\Sigma}} = \hat{\boldsymbol{R}}\boldsymbol{\Sigma}\hat{\boldsymbol{R}}^T$, with

$$\begin{aligned} \boldsymbol{\Sigma} &= \begin{bmatrix} 1 & 0 & 0 \\ 0 & 1 & 0 \\ 0 & 0 & -1 \end{bmatrix} \\ \hat{\boldsymbol{R}} &= \begin{bmatrix} \hat{\boldsymbol{f}}_u(\overline{u}, \overline{v}) & \hat{\boldsymbol{f}}_v(\overline{u}, \overline{v}) & \hat{\boldsymbol{f}}_u(\overline{u}, \overline{v}) \wedge \hat{\boldsymbol{f}}_v(\overline{u}, \overline{v}) \end{bmatrix} \\ \hat{\boldsymbol{t}} &= -\hat{\boldsymbol{R}}(\boldsymbol{\Sigma} - Id)\hat{\boldsymbol{R}}^T \boldsymbol{f}(\overline{u}\,\overline{v}) \end{aligned} \tag{21}$$

then $s \circ \boldsymbol{f}(u, v) = \hat{\boldsymbol{\Sigma}} \boldsymbol{f}(u, v) + \hat{\boldsymbol{t}}$ is the symmetric surface of $\boldsymbol{f}(u, v)$ with respect to a plane tangent to $\boldsymbol{f}(u, v)$ through the point $\boldsymbol{f}(\overline{u}, \overline{v})$.

Definition 3: A surface $\boldsymbol{h}(x, y)$ is said to be the *specular image* of a surface $\boldsymbol{f}(u, v)$ at a point $\boldsymbol{f}(\overline{u}, \overline{v})$ if there exist a rigid motion $g = (\boldsymbol{R}, \boldsymbol{z})$, a symmetry $s = (\hat{\boldsymbol{R}} \boldsymbol{\Sigma} \hat{\boldsymbol{R}}^T, \hat{\boldsymbol{t}})$ as in (21), and a diffeomorphism $\Phi: \mathbb{R}^2 \rightarrow \mathbb{R}^2$, $\Phi: (x, y) \mapsto (u, v)$ such that $g \circ \boldsymbol{h}(x, y) = s \circ \boldsymbol{f} \circ \Phi(x, y)$.

Notice explicitly that a surface and its specular image, as defined above, have a point in common, the mirror plane being the tangent plane at such contact point.

In the proof of theorem 1, the following lemma will be instrumental:

Lemma 3: If two surfaces are specular, the change of coordinates $\Phi: \mathbb{R}^2 \rightarrow \mathbb{R}^2$ in definition 3 is a map whose Jacobian $\boldsymbol{J}_\Phi$ has either of these forms:

$$\boldsymbol{J}_\Phi = \pm \begin{bmatrix} \dfrac{\|\boldsymbol{h}_x\|}{\|\boldsymbol{f}_u\|} & 0 \\ 0 & -\dfrac{\|\boldsymbol{h}_y\|}{\|\boldsymbol{f}_v\|} \end{bmatrix} \text{ or } \boldsymbol{J}_\Phi = \pm \begin{bmatrix} 0 & \dfrac{\|\boldsymbol{h}_x\|}{\|\boldsymbol{f}_v\|} \\ \dfrac{\|\boldsymbol{h}_y\|}{\|\boldsymbol{f}_u\|} & 0 \end{bmatrix}$$

Proof: Suppose $g \circ \boldsymbol{h}(x, y) = s \circ \boldsymbol{f} \circ \Phi(x, y)$, then

$$\begin{aligned} (g \circ \boldsymbol{h})_x &= (s \circ \boldsymbol{f} \circ \Phi)_x \Rightarrow \boldsymbol{R}\boldsymbol{h}_x = \hat{\boldsymbol{\Sigma}} \boldsymbol{f}_u u_x + \hat{\boldsymbol{\Sigma}} \boldsymbol{f}_v v_x \\ (g \circ \boldsymbol{h})_y &= (s \circ \boldsymbol{f} \circ \Phi)_y \Rightarrow \boldsymbol{R}\boldsymbol{h}_y = \hat{\boldsymbol{\Sigma}} \boldsymbol{f}_u u_y + \hat{\boldsymbol{\Sigma}} \boldsymbol{f}_v v_y. \end{aligned}$$

The condition of orthogonality of the local coordinates implies that the inner product $(\boldsymbol{R}\boldsymbol{h}_x)^T(\boldsymbol{R}\boldsymbol{h}_y) = \|\boldsymbol{f}_u\|^2 u_x u_y + \|\boldsymbol{f}_v\|^2 v_x v_y$ is zero. Hence the three conditions $u_x u_y = 0$, $v_x v_y = 0$ and $\mathtt{rank}(J_\Phi) = 2$ together gives either $u_x, v_y \neq 0$, $u_y = v_x = 0$ or $u_x = v_y = 0$, $u_y, v_x \neq 0$. Suppose the first case holds. The inner and cross products of both sides are evaluated, recalling that $\det(\hat{\boldsymbol{\Sigma}}) = -1$, as

$$\begin{aligned} \|\boldsymbol{h}_x\|^2 &= \|\boldsymbol{f}_u\|^2 u_x^2 \\ \|\boldsymbol{h}_y\|^2 &= \|\boldsymbol{f}_v\|^2 v_y^2 \\ \boldsymbol{R}(\boldsymbol{h}_x \wedge \boldsymbol{h}_y) &= -u_x v_y \hat{\boldsymbol{\Sigma}}(\boldsymbol{f}_u \wedge \boldsymbol{f}_v), \end{aligned}$$

hence

$$|u_x| = \frac{\|\boldsymbol{h}_x\|}{\|\boldsymbol{f}_u\|}; \quad |v_y| = \frac{\|\boldsymbol{h}_y\|}{\|\boldsymbol{f}_v\|}. \tag{22}$$

The sign of the components of $\boldsymbol{J}_\Phi$ is derived considering the convention of outwardly pointing normals. This implies $-1 = (\hat{\boldsymbol{f}}_u \wedge \hat{\boldsymbol{f}}_v)^T \boldsymbol{R}(\hat{\boldsymbol{h}}_x \wedge \hat{\boldsymbol{h}}_y) = -(\hat{\boldsymbol{f}}_u \wedge \hat{\boldsymbol{f}}_v)^T \hat{\boldsymbol{\Sigma}}(\hat{\boldsymbol{f}}_u \wedge \hat{\boldsymbol{f}}_v)(u_x v_y/|u_x||v_y|)$. Using the fact that $(\hat{\boldsymbol{f}}_u \wedge \hat{\boldsymbol{f}}_v)^T \hat{\boldsymbol{\Sigma}}(\hat{\boldsymbol{f}}_u \wedge \hat{\boldsymbol{f}}_v) = -1$, we get $(u_x v_y/|u_x||v_y|) = -1$, hence u_x, v_y have opposite signs and $\boldsymbol{J}_\Phi$ has the first of the two forms in the lemma statement.

If instead $u_x = v_y = 0$, $u_y, v_x \neq 0$, similar arguments can be used to prove that $\boldsymbol{J}_\Phi$ has the second form. ■

We are now in a position to prove Theorem 1.

Proof: Part 1: Holonomy $\Leftarrow$ Specularity.

The control vector fields in (13) are written explicitly as

$$\boldsymbol{g}_1 = \begin{bmatrix} \dfrac{1}{\|\boldsymbol{f}_u\|} \\ 0 \\ \dfrac{\cos\psi}{\|\boldsymbol{h}_x\|} \\ \dfrac{-\sin\psi}{\|\boldsymbol{h}_y\|} \\ \hat{t}_1 \end{bmatrix} \quad \text{and} \quad \boldsymbol{g}_2 = \begin{bmatrix} 0 \\ \dfrac{1}{\|\boldsymbol{f}_v\|} \\ \dfrac{-\sin\psi}{\|\boldsymbol{h}_x\|} \\ \dfrac{-\cos\psi}{\|\boldsymbol{h}_y\|} \\ \hat{t}_2 \end{bmatrix}$$

where

$$\begin{aligned} \hat{t}_1 &= t_1 + \cos\psi \tilde{t}_1 - \sin\psi \tilde{t}_2 \\ \hat{t}_2 &= t_2 - \sin\psi \tilde{t}_1 - \cos\psi \tilde{t}_2 \\ t_1 &= \frac{\boldsymbol{f}_v^T \boldsymbol{f}_{uu}}{\|\boldsymbol{f}_u\|^2 \|\boldsymbol{f}_v\|} \\ t_2 &= \frac{\boldsymbol{f}_v^T \boldsymbol{f}_{uv}}{\|\boldsymbol{f}_u\| \|\boldsymbol{f}_v\|^2} \\ \tilde{t}_1 &= \frac{\boldsymbol{h}_y^T \boldsymbol{h}_{xx}}{\|\boldsymbol{h}_x\|^2 \|\boldsymbol{h}_y\|} \\ \tilde{t}_2 &= \frac{\boldsymbol{h}_y^T \boldsymbol{h}_{xy}}{\|\boldsymbol{h}_x\| \|\boldsymbol{h}_y\|^2}. \end{aligned}$$

The Lie bracket $\boldsymbol{g}_3 = [\boldsymbol{g}_1, \boldsymbol{g}_2]$ is evaluated as shown in (23) at the bottom of the page, where by t_{iz} we denote the derivative of t_i with respect to the variable z. It will be shown below that $\boldsymbol{g}_3 = -t_1 \boldsymbol{g}_1 - t_2 \boldsymbol{g}_2$ at a specular configuration.

$$\boldsymbol{g}_3 = \begin{bmatrix} -\dfrac{t_1}{\|\boldsymbol{f}_u\|} \\ -\dfrac{t_2}{\|\boldsymbol{f}_v\|} \\ \dfrac{1}{\|\boldsymbol{h}_x\|}\left(\tilde{t}_1 - \cos\psi \hat{t}_1 + \sin\psi \hat{t}_2\right) \\ \dfrac{1}{\|\boldsymbol{h}_y\|}\left(\tilde{t}_2 + \sin\psi \hat{t}_1 + \cos\psi \hat{t}_2\right) \\ \dfrac{t_{2u}}{\|\boldsymbol{f}_u\|} - \dfrac{t_{1v}}{\|\boldsymbol{f}_v\|} - \dfrac{\tilde{t}_{2x}}{\|\boldsymbol{h}_x\|} + \dfrac{\tilde{t}_{1y}}{\|\boldsymbol{h}_y\|} - \hat{t}_1\left(\hat{t}_1 - t_1\right) - \hat{t}_2\left(\hat{t}_2 - t_2\right) \end{bmatrix} \tag{23}$$

In fact, the first two components trivially satisfy this condition. The third and fourth components do also, by simply observing that

$$\tilde{t}_1 - \hat{t}_1 \cos\psi + \hat{t}_2 \sin\psi = -t_1 \cos\psi + t_2 \sin\psi$$

and

$$\tilde{t}_2 + \hat{t}_1 \sin\psi + \hat{t}_2 \cos\psi = +t_1 \sin\psi + t_2 \cos\psi.$$

The last component of $\boldsymbol{g}_3$ satisfies the condition if the surfaces are specular. In this case, we know that there exists a change of coordinates Φ such that $g \circ \boldsymbol{h}(x, y) = s \circ \boldsymbol{f} \circ \Phi(x, y)$ with $\boldsymbol{J}_\Phi$ as in Lemma 3. If

$$\boldsymbol{J}_\Phi = \pm \begin{bmatrix} \frac{\|\boldsymbol{h}_x\|}{\|\boldsymbol{f}_u\|} & 0 \\ 0 & -\frac{\|\boldsymbol{h}_y\|}{\|\boldsymbol{f}_v\|} \end{bmatrix}$$

then

$$\begin{aligned} \boldsymbol{R}\boldsymbol{h}_x &= \frac{\|\boldsymbol{h}_x\|}{\|\boldsymbol{f}_u\|} \hat{\boldsymbol{\Sigma}} \boldsymbol{f}_u = \|\boldsymbol{h}_x\| \hat{\boldsymbol{\Sigma}} \hat{\boldsymbol{f}}_u \\ \boldsymbol{R}\boldsymbol{h}_y &= -\frac{\|\boldsymbol{h}_y\|}{\|\boldsymbol{f}_v\|} \hat{\boldsymbol{\Sigma}} \boldsymbol{f}_v = -\|\boldsymbol{h}_y\| \hat{\boldsymbol{\Sigma}} \hat{\boldsymbol{f}}_v \end{aligned}$$

and

$$\begin{aligned} (g \circ \boldsymbol{h})_{xx} &= \hat{\boldsymbol{\Sigma}} \hat{\boldsymbol{f}}_u \frac{\partial \|\boldsymbol{h}_x\|}{\partial x} + \|\boldsymbol{h}_x\| \hat{\boldsymbol{\Sigma}} \frac{\partial \hat{\boldsymbol{f}}_u}{\partial u} \\ (g \circ \boldsymbol{h})_{xy} &= \hat{\boldsymbol{\Sigma}} \hat{\boldsymbol{f}}_u \frac{\partial \|\boldsymbol{h}_x\|}{\partial y} + \|\boldsymbol{h}_x\| \hat{\boldsymbol{\Sigma}} \frac{\partial \hat{\boldsymbol{f}}_u}{\partial v} \end{aligned}$$

hence

$$\begin{aligned} \tilde{t}_1 &= \frac{\boldsymbol{h}_y^T \boldsymbol{h}_{xx}}{\|\boldsymbol{h}_y\| \|\boldsymbol{h}_x\|^2} = -\frac{\boldsymbol{f}_v^T \boldsymbol{f}_{uu}}{\|\boldsymbol{f}_v\| \|\boldsymbol{f}_u\|^2} = -t_1 \\ \tilde{t}_2 &=, \frac{\boldsymbol{h}_y^T \boldsymbol{h}_{xy}}{\|\boldsymbol{h}_y\|^2 \|\boldsymbol{h}_x\|} = \frac{\boldsymbol{f}_v^T \boldsymbol{f}_{uv}}{\|\boldsymbol{f}_v\|^2 \|\boldsymbol{f}_u\|} = t_2 \end{aligned} \tag{24}$$

and

$$\begin{aligned} \frac{t_{1v}}{\|\boldsymbol{f}_v\|} &= \frac{\tilde{t}_{1y}}{\|\boldsymbol{h}_y\|} \\ \frac{t_{2u}}{\|\boldsymbol{f}_u\|} &= \frac{\tilde{t}_{2x}}{\|\boldsymbol{h}_x\|}. \end{aligned} \tag{25}$$

If otherwise $\boldsymbol{J}_\Phi$ has the second form in the statement of Lemma 1, then, by similar calculations and taking into account that, because of the orthogonality of the parameterization, it holds $\boldsymbol{f}_u^T \boldsymbol{f}_{vv} = -\boldsymbol{f}_v^T \boldsymbol{f}_{uv}$ and $\boldsymbol{f}_u^T \boldsymbol{f}_{uv} = -\boldsymbol{f}_v^T \boldsymbol{f}_{uu}$, one gets

$$\begin{aligned} \tilde{t}_1 &= \frac{\boldsymbol{h}_y^T \boldsymbol{h}_{xx}}{\|\boldsymbol{h}_y\| \|\boldsymbol{h}_x\|^2} = \frac{-\boldsymbol{f}_v^T \boldsymbol{f}_{uv}}{\|\boldsymbol{f}_u\| \|\boldsymbol{f}_v\|^2} = -t_2 \\ \tilde{t}_2 &= \frac{\boldsymbol{h}_y^T \boldsymbol{h}_{xy}}{\|\boldsymbol{h}_y\|^2 \|\boldsymbol{h}_x\|} = \frac{-\boldsymbol{f}_v^T \boldsymbol{f}_{uu}}{\|\boldsymbol{f}_u\|^2 \|\boldsymbol{f}_v\|} = -t_1 \end{aligned} \tag{26}$$

and

$$\begin{aligned} \frac{t_{1v}}{\|\boldsymbol{f}_v\|} &= -\frac{\tilde{t}_{2x}}{\|\boldsymbol{h}_x\|} \\ \frac{t_{2u}}{\|\boldsymbol{f}_u\|} &= -\frac{\tilde{t}_{1y}}{\|\boldsymbol{h}_y\|} \end{aligned} \tag{27}$$

It should be noticed that either (24) and (25), or (26) and (27), hold true for all points in the neighborhood of the contact point where specularity holds. To verify that the last component of $\boldsymbol{g}_3$ in (23) is equal to $-t_1\hat{t}_1 - t_2\hat{t}_2$, it suffices to notice that, as a consequence of either (24) or (26), it holds

$$-\hat{t}_1 (\hat{t}_1 - t_1) - \hat{t}_2 (\hat{t}_2 - t_2) = -\hat{t}_1 t_1 - \hat{t}_2 t_2.$$

(end of Proof of the Part 1).

Part 2: Holonomy $\Rightarrow$ Specularity.

By hypothesis, the constraint equation (11) are integrable, i.e. there exists a two dimensional submanifold described by $\{\boldsymbol{q} \in \mathcal{M}: \boldsymbol{F}(\boldsymbol{q}) = 0\}$, with $\boldsymbol{F}$ a C^∞ map $\boldsymbol{F}: \mathbb{R}^2 \times \mathbb{R}^2 \times S^1 \to \mathbb{R}^2 \times S^1$ such that its rank-3 Jacobian is

$$D\boldsymbol{F} = \begin{bmatrix} \boldsymbol{M}_1 & -\boldsymbol{R}_\psi \boldsymbol{M}_2 & 0 \\ \boldsymbol{T}_1 \boldsymbol{M}_1 & \boldsymbol{T}_2 \boldsymbol{M}_2 & -1 \end{bmatrix}.$$

By the Implicit Function Theorem, there exists locally a C^∞ map $\hat{\Phi}$: $\mathbb{R}^2 \to \mathbb{R}^3$; $\hat{\Phi}(x, y) = (u, v, \psi)$ such that $\boldsymbol{F}(x, y, \hat{\Phi}(x, y)) = 0$. Let Φ denote the trivial restriction of $\hat{\Phi}$, Φ: $\mathbb{R}^2 \to \mathbb{R}^2$: $\Phi(x, y) = (u, v)$.

Consider the surface $\tilde{\boldsymbol{f}}(x, y) = s \circ \boldsymbol{f} \circ \Phi(x, y)$, which is the specular image of $\boldsymbol{f}(u, v)$ at point $(\overline{u}, \overline{v}) = \Phi(\overline{x}, \overline{y})$. The theorem will be proved by showing that the surface $\tilde{\boldsymbol{f}}(x, y)$ and $\boldsymbol{h}(x, y)$ are indeed the same.

The elements of the first fundamental form of $\tilde{\boldsymbol{f}}$are evaluated as

$$\begin{aligned} \tilde{\boldsymbol{f}}_x &= \hat{\boldsymbol{\Sigma}} \boldsymbol{f}_u \frac{\|\boldsymbol{h}_x\| \cos\psi}{\|\boldsymbol{f}_u\|} - \hat{\boldsymbol{\Sigma}} \boldsymbol{f}_v \frac{\|\boldsymbol{h}_x\| \sin\psi}{\|\boldsymbol{f}_v\|} \\ \tilde{\boldsymbol{f}}_y &= -\hat{\boldsymbol{\Sigma}} \boldsymbol{f}_u \frac{\|\boldsymbol{h}_y\| \sin\psi}{\|\boldsymbol{f}_u\|} - \hat{\boldsymbol{\Sigma}} \boldsymbol{f}_v \frac{\|\boldsymbol{h}_y\| \cos\psi}{\|\boldsymbol{f}_v\|} \\ \tilde{\boldsymbol{n}} &= \hat{\boldsymbol{\Sigma}} \frac{\boldsymbol{f}_u \wedge \boldsymbol{f}_v}{\|\boldsymbol{f}_u\| \|\boldsymbol{f}_v\|} \end{aligned}$$

which implies

$$\begin{aligned} \left\| \tilde{\boldsymbol{f}}_x \right\| &= \|\boldsymbol{h}_x\| \\ \left\| \tilde{\boldsymbol{f}}_y \right\| &= \|\boldsymbol{h}_y\| \end{aligned}$$

hence the first fundamental forms of $\tilde{\boldsymbol{f}}(x, y)$ and $\boldsymbol{h}(x, y)$ coincide, i.e.

$$\tilde{\mathcal{I}} = \mathcal{I}_2. \tag{28}$$

Further, it holds that

$$\begin{aligned} \tilde{\boldsymbol{n}}_x &= \hat{\boldsymbol{\Sigma}} \boldsymbol{n}_u \frac{\|\boldsymbol{h}_x\| \cos\psi}{\|\boldsymbol{f}_u\|} - \hat{\boldsymbol{\Sigma}} \boldsymbol{n}_v \frac{\|\boldsymbol{h}_x\| \sin\psi}{\|\boldsymbol{f}_v\|} \\ \tilde{\boldsymbol{n}}_y &= -\hat{\boldsymbol{\Sigma}} \boldsymbol{n}_u \frac{\|\boldsymbol{h}_y\| \sin\psi}{\|\boldsymbol{f}_u\|} - \hat{\boldsymbol{\Sigma}} \boldsymbol{n}_v \frac{\|\boldsymbol{h}_y\| \cos\psi}{\|\boldsymbol{f}_v\|}. \end{aligned}$$

The elements of the second fundamental form of $\tilde{\boldsymbol{f}}$ are evaluated as

$$\begin{aligned} -\tilde{\boldsymbol{n}}^T \tilde{\boldsymbol{f}}_{xx} &= \tilde{\boldsymbol{n}}_x^T \tilde{\boldsymbol{f}}_x \\ -\tilde{\boldsymbol{n}}^T \tilde{\boldsymbol{f}}_{yx} &= \tilde{\boldsymbol{n}}_x^T \tilde{\boldsymbol{f}}_y \\ -\tilde{\boldsymbol{n}}^T \tilde{\boldsymbol{f}}_{xy} &= \tilde{\boldsymbol{n}}_y^T \tilde{\boldsymbol{f}}_x \\ -\tilde{\boldsymbol{n}}^T \tilde{\boldsymbol{f}}_{yy} &= \tilde{\boldsymbol{n}}_y^T \tilde{\boldsymbol{f}}_y \end{aligned}$$

and, by some calculations, the relation between the second fundamental forms of $\tilde{\boldsymbol{f}}(x, y)$ and $\boldsymbol{f}(u, v)$ is found as

$$\tilde{\boldsymbol{M}}^{-1}\tilde{\mathcal{II}}\tilde{\boldsymbol{M}}^{-1} = \boldsymbol{R}_\psi \boldsymbol{M}_1^{-1}\mathcal{II}_1\boldsymbol{M}_1^{-1}\boldsymbol{R}_\psi \tag{29}$$

where $\tilde{\boldsymbol{M}} = \sqrt{\tilde{\mathcal{I}}}$.

The first and second fundamental forms $\mathcal{I}_2, \mathcal{II}_2$ for a surface $\boldsymbol{h}(x, y)$ holonomically rolling on $\boldsymbol{f}(u, v)$ are derived considering once again the rolling-without-sliding constraint (7) in the form (5), rewritten as

$$\begin{aligned} \hat{\boldsymbol{f}}_u \cos\psi - \hat{\boldsymbol{f}}_v \sin\psi &= \hat{\boldsymbol{h}}_x \\ -\hat{\boldsymbol{f}}_u \sin\psi - \hat{\boldsymbol{f}}_v \cos\psi &= \hat{\boldsymbol{h}}_y \end{aligned}$$

It directly follows that $\mathcal{I}_2 = \mathcal{I}_1$. Further, observing that

$$\begin{aligned} \dot{\boldsymbol{n}}_1^T \left(\hat{\boldsymbol{f}}_u \cos\psi - \hat{\boldsymbol{f}}_v \sin\psi\right) &= \dot{\boldsymbol{n}}_2^T \hat{\boldsymbol{h}}_x \\ \dot{\boldsymbol{n}}_1^T \left(-\hat{\boldsymbol{f}}_u \sin\psi - \hat{\boldsymbol{f}}_v \cos\psi\right) &= \dot{\boldsymbol{n}}_2^T \hat{\boldsymbol{h}}_y \end{aligned}$$

by some calculations one gets

$$\boldsymbol{M}_2^{-1}\mathcal{II}_2\boldsymbol{M}_2^{-1} = \boldsymbol{R}_\psi \boldsymbol{M}_1^{-1}\mathcal{II}_1\boldsymbol{M}_1^{-1}\boldsymbol{R}_\psi$$

where $\boldsymbol{M}_2 = \sqrt{\mathcal{I}_2}$. Therefore, as (28) implies $\tilde{\boldsymbol{M}} = \boldsymbol{M}_2$, we have

$$\tilde{\mathcal{II}} = \mathcal{II}_2. \tag{30}$$

Recalling from Bonnet's theorem [26] that two surfaces with equal fundamental forms coincide up to a rigid motion in $SE(3)$, it is proved that a surface S_2 rolling holonomically on S_1 must be specular of S_1 in a neighborhood of the contact point.

(end of Proof of Part 2).

Part 3: Nonspecularity $\Rightarrow$ Maximal Nonholonomy.

Because of Chow's theorem, we only need to show that $\dim\langle \boldsymbol{g}_1, \boldsymbol{g}_2 | \boldsymbol{g}_1, \boldsymbol{g}_2\rangle = 5$ in a neighborhood of a nonspecular configuration. From (23), the vector field $\boldsymbol{g}_3 = [\boldsymbol{g}_1, \boldsymbol{g}_2]$ at a generic configuration can be rewritten as $\boldsymbol{g}_3 = -t_1\boldsymbol{g}_1 - t_2\boldsymbol{g}_2 + \hat{\boldsymbol{g}}_3$, with $\hat{\boldsymbol{g}}_3 = [0 \quad 0 \quad 0 \quad 0 \quad \hat{t}_3]^T$, and $\hat{t}_3 = (t_{2u}/\|\boldsymbol{f}_u\|) - (t_{1v}/\|\boldsymbol{f}_v\|) - (\tilde{t}_{2x}/\|\boldsymbol{h}_x\|) + (\tilde{t}_{1y}/\|\boldsymbol{h}_y\|) - \hat{t}_1(\hat{t}_1 - 2t_1) - \hat{t}_2(\hat{t}_2 - 2t_2)$.

We have then

$$\begin{aligned} &\langle \boldsymbol{g}_1, \boldsymbol{g}_2 | \boldsymbol{g}_1, \boldsymbol{g}_2\rangle \\ &\quad \supseteq \operatorname{span}\{\boldsymbol{g}_1, \boldsymbol{g}_2, \boldsymbol{g}_3, [\boldsymbol{g}_1, \boldsymbol{g}_3], [\boldsymbol{g}_2, \boldsymbol{g}_3]\} \\ &\quad = \operatorname{span}\{\boldsymbol{g}_1, \boldsymbol{g}_2, \hat{\boldsymbol{g}}_3, [\boldsymbol{g}_1, \hat{\boldsymbol{g}}_3], [\boldsymbol{g}_2, \hat{\boldsymbol{g}}_3]\} \\ &\quad = \operatorname{span}\begin{bmatrix} \frac{1}{\|\boldsymbol{f}_u\|} & 0 & 0 & 0 & 0 \\ 0 & \frac{1}{\|\boldsymbol{f}_v\|} & 0 & 0 & 0 \\ \frac{\cos\psi}{\|\boldsymbol{h}_x\|} & \frac{-\sin\psi}{\|\boldsymbol{h}_x\|} & 0 & \frac{\sin\psi}{\|\boldsymbol{h}_x\|}\hat{t}_3 & \frac{\cos\psi}{\|\boldsymbol{h}_x\|}\hat{t}_3 \\ \frac{-\sin\psi}{\|\boldsymbol{h}_y\|} & \frac{-\cos\psi}{\|\boldsymbol{h}_y\|} & 0 & \frac{\cos\psi}{\|\boldsymbol{h}_y\|}\hat{t}_3 & \frac{-\sin\psi}{\|\boldsymbol{h}_y\|}\hat{t}_3 \\ \hat{t}_1 & \hat{t}_2 & \hat{t}_3 & \hat{t}_4 & \hat{t}_5 \end{bmatrix} \end{aligned} \tag{31}$$

with $\hat{t}_4 = (\hat{t}_{3u}/\|\boldsymbol{f}_u\|) + (\hat{t}_{3x}\cos\psi/\|\boldsymbol{h}_x\|) - (\hat{t}_{3y}\sin\psi/\|\boldsymbol{h}_y\|) - \hat{t}_{1\psi}\hat{t}_3$ and $\hat{t}_5 = (\hat{t}_{3v}/\|\boldsymbol{f}_v\|) - (\hat{t}_{3x}\sin\psi/\|\boldsymbol{h}_x\|) - (\hat{t}_{3y}\cos\psi/\|\boldsymbol{h}_y\|) - \hat{t}_{2\psi}\hat{t}_3$. For all ψ the matrix appearing in the last term of (31) can be put into diagonal form by elementary columns operations, and its eigenvalues are:

$$\begin{aligned} &\left\{\frac{1}{\|\boldsymbol{f}_u\|}, \frac{1}{\|\boldsymbol{f}_v\|}, \frac{\sin\psi}{\|\boldsymbol{h}_x\|}\hat{t}_3, \frac{-\hat{t}_3}{\|\boldsymbol{h}_y\|}, \hat{t}_3\right\}; \ \psi \neq \frac{k\pi}{2} \\ &\left\{\frac{1}{\|\boldsymbol{f}_u\|}, \frac{1}{\|\boldsymbol{f}_v\|}, \frac{\pm\hat{t}_3}{\|\boldsymbol{h}_x\|}, \frac{\pm\hat{t}_3}{\|\boldsymbol{h}_y\|}, \hat{t}_3\right\}; \ \psi = k\pi \\ &\left\{\frac{1}{\|\boldsymbol{f}_u\|}, \frac{1}{\|\boldsymbol{f}_v\|}, \frac{\mp\hat{t}_3}{\|\boldsymbol{h}_x\|}, \frac{\pm\hat{t}_3}{\|\boldsymbol{h}_y\|}, \hat{t}_3\right\}; \ \psi = \frac{k\pi}{2}. \end{aligned}$$

The matrix is always full rank whenever $\hat{t}_3 \neq 0$ (in which case the matrix has rank 2). Recalling from part 1 and 2 of this proof that the condition $\hat{t}_3 \equiv 0$ in a neighborhood of the contact point is equivalent to specularity of objects, the proof is finalized. ∎

Based on the above results, the structure of the reachable manifold of a system of relatively convex rolling bodies can be described as follows:

Case i) $\dim\langle \boldsymbol{g}_1, \boldsymbol{g}_2 | \boldsymbol{g}_1, \boldsymbol{g}_2\rangle = 5, \forall \boldsymbol{q} \in \mathcal{M}$: the whole $\mathcal{M}$ is reachable. This is the case with *almost* all pairs of strictly relatively convex bodies;

Case ii) $\dim\langle \boldsymbol{g}_1, \boldsymbol{g}_2 | \boldsymbol{g}_1, \boldsymbol{g}_2\rangle = 2, \forall \boldsymbol{q} \in \mathcal{M}$: the configuration manifold is foliated in two-dimensional maximal integral submanifolds. This is the case e.g. with two equal spheres rolling on each other.

Case iii) $\dim\langle \boldsymbol{g}_1, \boldsymbol{g}_2 | \boldsymbol{g}_1, \boldsymbol{g}_2\rangle$ varies on $\mathcal{M}$: There are connected 2-dimensional submanifolds $\mathcal{M}'_\ell \subset \mathcal{M}$ of specular configurations which are maximal integral submanifolds. In other words, every configuration $\boldsymbol{q}_1 \in \mathcal{M}'_\ell$ can be reached from $\boldsymbol{q}_0$ if and only if $\boldsymbol{q}_0 \in \mathcal{M}'_\ell$. The complement $\mathcal{M} \backslash \bigcup_\ell \mathcal{M}'_\ell$ is comprised of (possibly several, nonconnected) five-dimensional maximal integral submanifolds.

Example: The system of two identical rugby balls possesses ∞^2 two-dimensional and one five-dimensional maximal integral submanifolds. In fact, consider an initial configuration of the balls touching at their medium circle such that their axis of symmetry is parallel. This is a specular configuration, and the family of such configurations is clearly diffeomorphic to $S^1 \times S^1$. Indeed, they could be obtained by detaching the balls slightly, rotating either one about its symmetry axis, and bringing them back in contact. Rolling the balls arbitrarily, starting from any of these initial configurations, will keep the balls specular, generating orbits that can not intersect with those starting from a different initial condition of the described family. If starting from a nonspecular configuration, on the other hand, although local controllability is guaranteed, it will never be possible to reach a specular configuration.

Finally, for the sake of completeness, we report the following

Theorem 2: The rolling-without-sliding constraints (7) between two relatively strictly convex surfaces is maximally nonholonomic.

Proof: The proof directly follows from the computation of the Lie Algebra generated by the vector fields in (12), and is omitted here. ∎

IV. Planning Algorithm

It may be worthwhile noticing that, as a particular case of theorem 1, any convex body rolling on a flat surface is controllable.

Hence, the possibility of achieving dexterous robotic manipulation of arbitrary convex objects by means of a robotic hand with as few as three motors and flat fingers, is guaranteed in principle. To realize such principle, it is necessary that a mechanism for the hand can be designed that allows application of arbitrary angular velocities to the object. Two examples of such mechanisms are reported in Figs. 1 and 2. Notice that in practice, a fourth motor may be needed to keep hold of the manipulated object, and achieve sufficient friction forces to impart rolling motions.

To realize the goal of nonholonomic dextrous manipulation, several problems of both technological and theoretical nature remain to be solved. Among theoretical difficulties to be overcome, the two prominent ones are to find an efficient algorithm to steer the system between two given configurations (the *planning problem*), and providing feedback laws stabilizing motions in the presence of uncertainties. In this paper, we confine ourselves to describing a method for planning, and leave the control problem as a challenging open question.

Generally speaking, the problem of planning a driftless system

$$\dot{\boldsymbol{q}} = \boldsymbol{G}(\boldsymbol{q})\boldsymbol{w},\ \boldsymbol{q}(0) = \boldsymbol{q}_0 \in \mathbb{R}^n \tag{32}$$

consists in finding, for each pair $(\boldsymbol{q}_0, \boldsymbol{q}_f)$, a control function $\boldsymbol{w}$: $[0, 1] \rightarrow \mathbb{R}^m$, $t \mapsto \boldsymbol{w}(t)$ within an admissible set W such that, for the corresponding solution $\boldsymbol{q}(t, \boldsymbol{q}_0, \boldsymbol{w})$ of (32), it holds $\boldsymbol{q}(1, \boldsymbol{q}_0, \boldsymbol{w}) = \boldsymbol{q}_f$. A brute force approach to this problem consists in:

1) solving (32) for a generic input $\boldsymbol{w}(\boldsymbol{p}, t)$ in a sufficiently general family $\overline{W} \subset W$ suitably parameterized by $\boldsymbol{p} \in \mathbb{R}^p$, and
2) solve the set of n nonlinear equations $\boldsymbol{q}(1, \boldsymbol{x}_0, \boldsymbol{p}) = \boldsymbol{q}_f$ in the p unknowns $\boldsymbol{p}$.

Obviously, both steps may possibly hide enormous difficulties, as solving an O.D.E. in closed form[1] is rarely possible, and solving large systems of nonlinear equations is notoriously hard. Indeed, the mathematically interesting problem behind planning is not to solve steps 1) or 2) above, but rather to find a feedback equivalence (i.e., a change of coordinates and a state feedback law) such that steps 1) and 2) become easily solvable.

As mentioned in the introduction, while there exist efficient planning algorithms for systems that are feedback equivalent to chained or nilpotent forms, only iterative planning schemes (such as the generic loops method of Sontag [27], or the continuation method of Sussmann and Chitour [28]) exist for general nonholonomic systems. Because of their generality, such schemes offer limited performance in computational terms, and algorithms that are more efficient should be sought that exploit any structure of the model at hand.

Although the kinematics of rolling bodies (13) do not fall in any of the categories to which the specialized, efficient algorithms mentioned above apply, they do possess an interesting property when one of the bodies has planar surface (as it happens, e.g., in the dexterous grippers of Figs. 1 and 2). In fact, the following proposition was shown to hold in [29]:

[1]The meaning of "closed" or "symbolic" form solution is not well defined. What is basically meant here is "easily computable."

Theorem 3: The kinematic equations (13) of a strictly convex body rolling on a planar surface are feedback equivalent to a strictly triangular form.

In other words, for (13) with say surface 2 a planar surface (i.e., $\boldsymbol{M}_2 = \boldsymbol{I}_{2\times 2}, \boldsymbol{T}_2 = \boldsymbol{0}_{1\times 2}, \boldsymbol{K}_2 = \boldsymbol{0}_{2\times 2}$), there exist a regular static state feedback $\boldsymbol{w} = \boldsymbol{A}(\boldsymbol{q})\hat{\boldsymbol{w}}$ and a state diffeomorphism $\boldsymbol{z} = \Phi(\boldsymbol{q})$ (actually, a simple reordering of coordinates with $\boldsymbol{z} = [u, v, \psi, x, y]^T$) such that

$$\dot{\boldsymbol{z}} = (\Phi_* \boldsymbol{G}\boldsymbol{A})|_{\boldsymbol{q}=\Phi^{-1}(\boldsymbol{z})}\, \hat{\boldsymbol{w}} = \begin{bmatrix} \boldsymbol{I}_{2\times 2} \\ \boldsymbol{T}_1\boldsymbol{M}_1 \\ \boldsymbol{R}_\psi \boldsymbol{M}_1 \end{bmatrix} \hat{\boldsymbol{w}}. \tag{33}$$

The relevance of strict triangular forms to planning is twofold. In fact, an O.D.E. in strictly triangular form can be easily solved by quadratures, i.e. the flow of the control vector fields is found simply by subsequently integrating their components over time. Furthermore, strict triangularity allows to break the solution of the system of n nonlinear equations of step 2) of the generic algorithm above, into the solution of multiple systems of fewer equations.

These advantages of the form (33) are exploited in the following algorithm. The algorithm will be illustrated referring to the case of a convex object rolling on a plate, whose surface is described in spherical coordinates as $\boldsymbol{f}$: $[-\pi, \pi) \times (-\pi/2, \pi/2) \rightarrow \mathbb{R}^3$,

$$\boldsymbol{f}(u, v) = \begin{bmatrix} \rho(u, v) \cos u \cos v \\ \rho(u, v) \sin u \cos v \\ \rho(u, v) \sin v \end{bmatrix}.$$

For objects with an axis of symmetry, which we consider henceforth for simplicity, spherical coordinates can be chosen such that they are everywhere orthogonal (except at the north and south pole singularities) and $\rho_u \equiv 0$. The strictly triangular form (33) reads in this case as

$$\dot{\boldsymbol{z}} = \begin{bmatrix} 1 & 0 \\ 0 & 1 \\ \dfrac{\rho \sin v - \rho_v \cos v}{\sqrt{\rho^2 + \rho_v^2}} & 0 \\ \rho \cos v \cos \psi & -\sqrt{\rho^2 + \rho_v^2} \sin \psi \\ \rho \cos v \sin \psi & -\sqrt{\rho^2 + \rho_v^2} \sin \psi \end{bmatrix} \hat{\boldsymbol{w}}. \tag{34}$$

A possible choice for the admissible input set U is to consider piecewise constant inputs over time intervals T with an alternating pattern,

$$\hat{\boldsymbol{w}}(kT + t) = \hat{\boldsymbol{w}}_k = \begin{cases} [\lambda_k, 0]^T & k \text{ even} \\ [0, \lambda_k]^T & k \text{ odd} \end{cases} \qquad 0 \le t < T$$

such that the flows $\Phi_{\boldsymbol{g}_i}^{\lambda_k T}$ of the two control vector fields are followed sequentially N times ($k = 0, 1, \cdots, N-1$). The flows can be integrated explicitly starting from initial conditions $\boldsymbol{z}_k = \boldsymbol{z}(kT)$ for k even as

$$\boldsymbol{z}_{k+1} = \begin{bmatrix} \lambda_k T + u_k \\ v_k \\ \Gamma(v_k)\lambda_k T + \psi_k \\ \dfrac{\rho \cos v_k}{\Gamma(v_k)} (\sin \psi_{k+1} - \sin \psi_k) + x_k \\ \dfrac{\rho \cos v_k}{\Gamma(v_k)} (\cos \psi_{k+1} - \cos \psi_k) + y_k. \end{bmatrix} \tag{35}$$

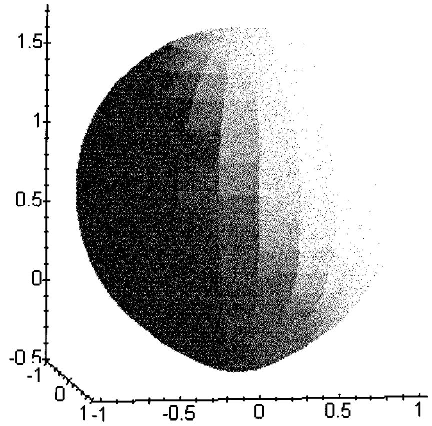

Fig. 4. Shape of the convex object used in the example.

where

$$\Gamma(v_k) = \left. \frac{\rho \sin v - \rho_v \cos v}{\sqrt{\rho^2 + \rho_v^2}} \right|_{v_k}$$

and for k odd as

$$z_{k+1} = \begin{bmatrix} u_k \\ \lambda_k T + v_k \\ \psi_k \\ -\lambda_k \sin \psi_k \Delta_k + x_k \\ -\lambda_k \cos \psi_k \Delta_k + y_k \end{bmatrix} \tag{36}$$

with

$$\Delta_k = \int_{kT}^{(k+1)T} \sqrt{\rho^2 + \rho_v^2}\, dt.$$

In terms of these positions, the planning problem can be restated as:

Problem 1: Given a pair (z_0, z_f), find an integer N and an N-tuple of real numbers $(\lambda_0, \cdots, \lambda_{N-1})$ such that the nonlinear, discrete-time system defined by (35), (36), with $z(0) = z_0$, has $z(N) = z_f$.

A solution to this problem is provided by the following algorithm, which exploits the strictly triangular structure of (34):

Algorithm

Step 1) Apply first inputs that take the first two variables to the desired value: set $\lambda_0 = \mu_0 = (u_f - u_0)/T$, $\lambda_1 = \mu_1 = (v_f - v_0)/T$, such that $z(2T) = [u_f, v_f, \psi_2, x_2, y_2]$;

Step 2) Apply a sequence of five inputs that does not alter the first two variables, i.e. $(\lambda_2 = 0, \lambda_3 = \mu_2, \lambda_4 = \mu_3, \lambda_5 = -\mu_2, \lambda_6 = -\mu_3)$[2] . By choosing

$$\mu_3 = \frac{\psi_f - \psi_2}{(\Gamma(v_4) - \Gamma(v_6))\,T},$$

with μ_2 arbitrary [provided that $\Gamma(v_4) \neq \Gamma(v_6)$], the third variable reaches its desired value: $z(6T) = [u_f, v_f, \psi_f, x_6, y_6]$;

Step 3) Apply a sequence of 15 controls that does not alter the first three variables, namely $(\lambda_7 = 0, \lambda_8 = \mu_4, \lambda_9 = \mu_5, \lambda_{10} = -\mu_4, \lambda_{11} = -\mu_5 + \mu_6, \lambda_{12} = \mu_7, \lambda_{13} = -\mu_6, , \lambda_{14} = -\mu_7, \lambda_{15} = \mu_5, \lambda_{16} = \mu_4, \lambda_{17} = -\mu_5, \lambda_{18} = -\mu_4 + \mu_7, \lambda_{19} = \mu_6, \lambda_{20} = -\mu_7, \lambda_{21} = -\mu_6$. For such a sequence to take the last two variables to their desired value, it is sufficient to choose any quadruple $(\mu_4, \mu_5, \mu_6, \mu_7)$ solving the system of two nonlinear algebraic equations $x_{22}(z_6, \mu_4, \mu_5, \mu_6, \mu_7) = x_f$; $y_{22}(z_6, \mu_4, \mu_5, \mu_6, \mu_7) = y_f$.

[2]The void input $\lambda_2 = 0$ is included for preserving consistency of index parity with (35) and (36), and of course it is not necessary to wait for the corresponding interval T before applying the next input.

Remark 2: The algorithm description highlights the role of commutator sequences of type $(ABA^{-1}B^{-1})$[3] in planning the input (a simple commutator is used at step 2, and a commutator of commutators at step 3). The final sequence of steps can however be written more compactly by imposing some further conditions, reducing the redundancy of solutions to the equations in step 3 but not compromising generality:

A) If $v_f \neq v_0$, setting $\mu_2 = -\mu_1$, $\mu_4 = \mu_3$, and $\mu_5 = \mu_6$, a control sequence is obtained $(\mu_0 + \mu_3, \mu_1 + \mu_5, -\mu_3 + \mu_7, -\mu_5, -\mu_7, \mu_5, \mu_3, -\mu_5, -\mu_3 + \mu_7, \mu_5, -\mu_7, -\mu_5)$, with $\mu_0 = (u_f - u_0)/T$, $\mu_1 = (v_f - v_0)/T$, $\mu_3 = (\psi_f - \psi_0 - \Gamma(v_0)\mu_0/(\Gamma(v_0) - \Gamma(v_0 + \mu_1 T))T)$, μ_5 and μ_7 solving the system of two nonlinear algebraic equations $x_{12}(z_0, \mu_5, \mu_7) = x_f$; $y_{12}(z_0, \mu_5, \mu_7) = y_f$, that steers from z_0 to z_f in just $12T$;

B) If otherwise $v_f = v_0$, the control sequence $(\nu_0 + \nu_1, \nu_2, -\nu_1 + \nu_3, -\nu_2 + \nu_4, -\nu_3, -\nu_4, \nu_3, \nu_2, -\nu_3, -\nu_2 + \nu_4, \nu_3, -\nu_4, -\nu_3)$, with $\nu_0 = (u_f - u_0)/T$, $\nu_1 = (\psi_f - \psi_0 - \Gamma(v_0)\nu_0/(\Gamma(v_0) - \Gamma(v_2))T)$, ν_2 arbitrary provided that $\Gamma(v_0) \neq \Gamma(v_2)$, ν_3 and ν_4 solving the system of two nonlinear algebraic equations $x_{13}(z_0, \nu_3, \nu_4) = x_f$; $y_{13}(z_0, \nu_3, \nu_4) = y_f$, steers the system in $13T$.

Example: As an example of application of the planning algorithm, consider the problem of rolling an object of general shape described in spherical coordinates by a weighted sum of suitable basis functions. In particular, recalling that spherical harmonics form a complete orthogonal basis for the space of L_2 functions on a spherical domain, one can write

$$\rho(v) = \sum_{\ell=0}^{n} \sum_{s=-\ell}^{\ell} f_{\ell s} Y_{\ell s}(v) \tag{37}$$

where f_{ls} are weights, and

$$\begin{aligned} Y_{\ell s}(u, v) &= U_{\ell s} \cos(us) P_\ell^s(\sin v) \qquad 0 < s \leq \ell \\ &= U_{\ell s} \sin(us) P_\ell^{|s|}(\sin v) \qquad -\ell \leq s < 0 \\ &= U_{\ell 0} P_\ell(\sin v) \qquad s = 0 \end{aligned}$$

[3]The inverse A^{-1} of an input A: $[0, T_A] \rightarrow \mathbb{R}_m$ is defined here as $A^{-1} = -A(T_A - t)$.

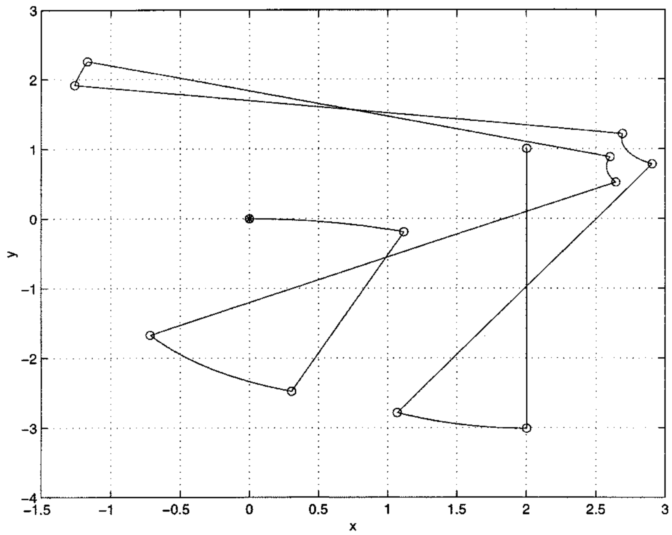

Fig. 5. Trajectory followed by the contact point on the plane for the planning example. Circles denote the states at the end of each planning interval; an asterisk denotes the initial conditions.

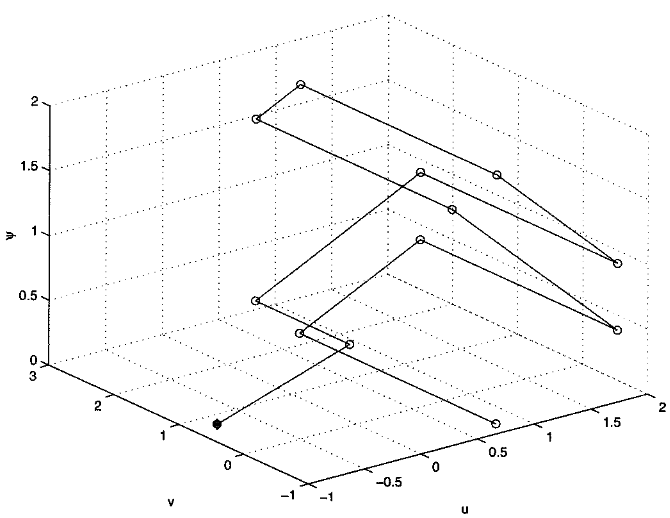

Fig. 6. Plot of the state variables $u,\ v,\ \psi$ in the planning example.

for $\ell = 0,\ 1,\ \cdots$. Here,

$$U_{\ell s} = \begin{cases} \sqrt{2}\sqrt{\dfrac{2\ell+1}{4\pi}\,\dfrac{(\ell-|s|)!}{(\ell+|s|)!}} & s \neq 0 \\ \sqrt{\dfrac{2\ell+1}{4\pi}} & s = 0 \end{cases}$$

$P_\ell,\ \ell = 0,\ 1,\ \cdots$, are the Legendre polynomials, and P_ℓ^s are the Legendre functions

$$P_\ell^s(z) = (1-z^2)^{s/2}\,\frac{\partial^s}{\partial z^s}\,P_\ell(z).$$

Observe that objects with an axial symmetry can be written with $f_{\ell,s} = 0,\ \forall s \neq 0$.

In Fig. 4 is reported the shape of an object obtained as the sum of the first three harmonics, with $f_{0,0} = 1,\ f_{1,0} = 0.4,\ f_{2,0} = 0.1$. The inputs resulting from application of the above algorithm, modified as in Remark 2-A, to the problem of steering from $\boldsymbol{z}_0 = (-\pi/4,\ \pi/4,\ 0,\ 0,\ 0)$ to $\boldsymbol{z}_f = (\pi/4,\ -\pi/4,\ 0,\ 2,\ 1)$, are computed as $\mu_0 = \pi/2,\ \mu_1 = -\pi/2,\ \mu_3 = -0.40;\ \mu_5 = 3.03;\ \mu_7 = 1.07$. The solution of the system of nonlinear equations at the last step of the algorithm is performed numerically. The path followed by the coordinates along the 12 intervals used for planning are reported in Figs. 5 and 6.

V. Conclusion

We have shown that almost all contacting pairs of bodies with regular surface can be brought to an arbitrary relative configuration by rolling. This is the proof of a conjecture that was advanced to justify construction of dextrous robotic hands with reduced hardware complexity. Furthermore, we presented a planning algorithm for a rather general class of objects rolling on a plane.

Several generalizations of the problem considered in this paper are practically relevant and present challenging open issues, of which we mention a few: firstly, paths planned by our algorithm may turn out to be rather long and complicated for some objects and configurations. Efficient algorithms to find optimal controls resulting in shortest paths, generalizing the work of [22] to generic objects, would be very useful. Work in this direction is reported in [30], who also derive controllability conditions equivalent to ours in an elegant coordinate-free setting. Secondly, if the object shape is not known beforehand, identification techniques need to be applied based on outputs from tactile sensors on the hand (see [31]), and adaptation mechanisms for re-planning paths should be devised. Thirdly, if objects to be manipulated do not possess a regular surface, tools adopted in this paper do not apply. In fact, quite different behaviors may appear, such as nondensity of the reachable set, that have been studied in [32]. Finally, feedback stabilization of a configuration of the manipulated object is an open problem which, due to the nonflatness of the system, appears to be rather hard to solve.

Appendix
Classification of Admissible Rolling Pairs

Consider the diagonal decomposition of the curvature forms

$$\boldsymbol{K}_1 = \boldsymbol{Q}_1\begin{bmatrix} k_1 & 0 \\ 0 & k_2 \end{bmatrix}\boldsymbol{Q}_1^T \quad \boldsymbol{K}_2 = \boldsymbol{Q}_2\begin{bmatrix} h_1 & 0 \\ 0 & h_2 \end{bmatrix}\boldsymbol{Q}_2^T$$
$$\boldsymbol{Q}_1^T\boldsymbol{R}_\psi\boldsymbol{Q}_2 = \begin{bmatrix} a & -b \\ -b & -a \end{bmatrix}$$

with $(k_1,\ k_2)$, $(h_1,\ h_2)$ the principal curvatures of the first and the second object. Assume the eigenvalues are ordered so that $k_1 \geq k_2;\ h_1 \geq h_2;\ k_1 \geq h_1$. The relative curvature form $\boldsymbol{K}_R$ is given by

$$\boldsymbol{K}_R = \boldsymbol{Q}_1\left(\begin{bmatrix} k_1+h_1 & 0 \\ 0 & k_2+h_2 \end{bmatrix} - b(h_1-h_2)\begin{bmatrix} b & -a \\ -a & -b \end{bmatrix}\right)\boldsymbol{Q}_1^T$$

The following cases apply:

TABLE II
CLASSIFICATION OF ADMISSIBLE ROLLING CONTACTS

Sign of principal curvature				Example	d.o.f.
h_2	h_1	k_2	k_1	$\forall\psi$	
-	-	+	+	sphere inside hollow sphere	2
-	0	+	+	sphere inside hollow cylinder	2
-	+	+	+	sphere onto saddle	2
0	+	+	+	sphere onto cylinder	2
+	+	+	+	sphere onto sphere	2
h_2	h_1	k_2	k_1	$\exists\psi$	
-	-	+	+	ellipsoid inside hollow ellipsoid	2
-	0	+	+	ellipsoid inside hollow cylinder	2
-	+	-	+	saddle onto saddle	2
-	+	0	+	cylinder onto saddle	2
-	+	+	+	ellipsoid onto saddle	2
0	+	0	+	cylinder onto cylinder	2
0	+	-	+	saddle onto cylinder	2
+	+	-	+	saddle onto ellipsoid	2
h_2	h_1	k_2	k_1	$\forall\psi$	
0	0	0	+	cylinder onto plane	1
h_2	h_1	k_2	k_1	$\exists\psi$	
-	0	0	+	cylinder inside hollow cylinder	1
-	+	-	+	ruled saddle onto ruled saddle	1
-	+	0	+	cylinder onto ruled saddle	1
0	+	-	+	ruled saddle onto cylinder	1
0	+	0	+	cylinder onto cylinder	1

A) Surfaces have an isolated contact point and have two rolling DOF.'s iff

$$
\begin{aligned}
\det \boldsymbol{K}_R &= (k_1+h_1)(k_2+h_2)+b^2(k_1-k_2)(h_1-h_2) > 0\\
\boldsymbol{K}_R^{11} &= (k_1+h_1)-b^2(h_1-h_2) > 0\\
\boldsymbol{K}_R^{22} &= (k_2+h_2)+b^2(h_1-h_2) > 0
\end{aligned}
$$

where $\boldsymbol{K}_R^{ij}$ denotes the i, jth element of matrix $\boldsymbol{K}_R$. These conditions hold $\forall\psi$ iff $-h_1 \le -h_2 < k_2 \le k_1$. They hold for some values of ψ iff $-h_1 < k_2 \le -h_2 < k_1$.

B) Surfaces have a one-dimensional contact manifold iff

B-i)

$$
\begin{aligned}
\det \boldsymbol{K}_R &= (k_1+h_1)(k_2+h_2)+b^2(k_1-k_2)(h_1-h_2) = 0\\
\boldsymbol{K}_R^{11} &= (k_1+h_1)-b^2(h_1-h_2) > 0\\
\boldsymbol{K}_R^{22} &= (k_2+h_2)+b^2(h_1-h_2) \ge 0
\end{aligned}
$$

or

B-ii)

$$
\begin{aligned}
\det \boldsymbol{K}_R &= (k_1+h_1)(k_2+h_2)+b^2(k_1-k_2)(h_1-h_2) = 0\\
\boldsymbol{K}_R^{11} &= (k_1+h_1)-b^2(h_1-h_2) = 0\\
\boldsymbol{K}_R^{22} &= (k_2+h_2)+b^2(h_1-h_2) > 0
\end{aligned}
$$

Case B-i) holds $\forall\psi$ iff $-h_1 = -h_2 = k_2 < k_1$; $\forall\psi \neq \pm(\pi/2)$ iff $-h_1 < -h_2 = k_2 = k_1$; and for $\psi = \{0, \pi\}$ iff $-h_1 < -h_2 = k_2 < k_1$. Case B-ii) holds for $\psi = \pm(\pi/2)$ iff $-h_1 < k_2 \le -h_2 = k_1$. Moreover, if surfaces have one rolling DOF., then $h_1 h_2 \le 0$ and $k_1 k_2 \le 0$ (contact points must be hyperbolic or parabolic).

Possible cases and examples are summarized in Table II, where the number of DOFs of rolling refers to enforcing both constraints (6) and (10).

ACKNOWLEDGMENT

The authors wish to thank Y. Chitour and S. S. Sastry for early cooperative work on this subject and many fruitful discussions. The role of R. Brockett in suggesting this direction of research in dextrous manipulation is also gratefully acknowledged.

REFERENCES

[1] J. Baillieul, "Open-loop control using oscillatory inputs," in *The Contr. Handbook*, W. S. Levine, Ed. Boca Raton, FL: CRC Press, 1996, ch. 57.7, pp. 967–980.
[2] I. Kolmanovsky and N. H. McClamroch, "Developments in nonholonomic control problems," *IEEE Contr. Syst. Mag.*, vol. 15, no. 6, pp. 20–36, 1995.
[3] R. W. Brockett, "On the rectification of vibratory motion," *Sensors and Actuators*, vol. 20, pp. 91–96, 1989.
[4] Y. Nakamura and R. Mukherjee, "Exploiting nonholonomic redundancy of free flying space robots," *IEEE Trans. Robot. Automat.*, vol. 9, no. 4, pp. 499–506, 1993.
[5] J. Ostrowski and J. Burdick, "Geometric perspectives on the mechanics and control of robotic locomotion," in *Robot. Res.: The Seventh Int Symp.*, G. Giralt and G. Hirzinger, Eds. New York: Springer Verlag, 1996, pp. 536–547.
[6] O. J. Sørdalen and Y. Nakamura, "Design of a nonholonomic manipulator," in *Proc. Int. Conf. on Robot. Automat.*, 1994, pp. 8–13.
[7] A. Bicchi and R. Sorrentino, "Dexterous manipulation through rolling," in *Proc. Int. Conf. Robot. Automat.*, 1995, pp. 452–457.
[8] A. Cole, J. Hauser, and S. S. Sastry, "Kinematics and control of a multifingered robot hand with rolling contact," *IEEE Trans. Automat. Contr.*, vol. 34, no. 4, pp. 398–404, 1989.
[9] R. W. Brockett, "Asymptotic stability and feedback stabilization," in *Diff. Geomet. Contr. Theory*, R. W. Brockett, G. A. Millmann, and H. Sussmann, Eds: Birkhäuser, 1982, pp. 181–191.
[10] R. M. Murray, "Nilpotent bases for a class of nonintegrable distributions with applications to trajectory generation for nonholonomic systems," *Math. Contr.Sig. Syst.*, vol. 7, pp. 58–75, 1994.
[11] D. Tilbury, R. M. Murray, and S. S. Sastry, "Trajectory generation for the n-trailer problem using goursat normal form," *IEEE Trans. Automat. Contr.*, vol. 40, no. 5, pp. 802–819, 1995.
[12] O. J. Sørdalen, "Conversion of the kinematics of a car with n trailers into a chained form," in *Proc. Int. Conf. Robot. Automat.*, 1993, pp. 382–387.
[13] R. Brockett and L. Dai, "Nonholonomic kinematics and the role of elliptic functions in constructive controllability," in *Nonholonomic Motion Planning*, Z. Li and J. F. Canny, Eds. Norwell, MA: Kluwer , 1993, pp. 1–21.
[14] R. M. Murray and S. S. Sastry, "Nonholonomic motion planning: Steering using sinusoids," *IEEE Trans. Automat. Contr.*, vol. 38, pp. 700–716, 1993.
[15] G. Lafferriere and H. Sussmann, "Motion planning for controllable systems without drift," in *Proc. Int. Conf. Robot. Automat.*, 1991, pp. 1148–1153.
[16] S. Monaco and D. Normand-Cyrot, "An introduction to motion planning under multirate digital control," in *Proc. 31st IEEE Int. Conf. Dec. Contr.*, 1992, pp. 1780–1785.
[17] G. Jacobs, "Motion planning by piecewise constant or polynomial inputs," in *Proc. Nonlinear Contr. Syst. Des. Symp. (NOLCOS)*, 1992, pp. 628–633.
[18] P. Rouchon, M. Fliess, J. Lèvine, and P. Martin, "Flatness, motion planning and traile systems," in *Proc. 32nd IEEE Int. Conf. Dec. Contr.*, 1993, pp. 2700–2705.
[19] A. Chelouah, "Exensions of differentially flat fields and liouvillian systems," in *Proc. 36th IEEE Int. Conf. Dec. Contr.*, 1997, pp. 4268–4273.
[20] D. J. Montana, "The kinematics of contact and grasp," *Inter. J. Robot. Res.*, vol. 7, no. 3, pp. 17–32, 1988.
[21] Z. Li and J. Canny, "Motion of two rigid bodies with rolling constraint," *IEEE Trans.Robot. Automat..*, vol. 6, no. 1, pp. 62–72, 1990.

[22] V. Jurdjevic, “The geometry of the plate-ball problem,” *Arch. Ratio. Mech. Anal.*, no. 124, pp. 305–328, 1993.
[23] M. Levi, “Geometric phases in the motion of rigid bodies,” *Arch. Ratio. Mech. Anal.*, no. 122, pp. 213–229, 1993.
[24] R. M. Murray, Z. Li, and S. S. Sastry, *Robot. Manip.: A Mathematical Intro*. Boca Raton, FL: CRC Press, 1994.
[25] H. Sussmann, “Orbits of families of vector fields and integrability of distributions,” *Trans. Am. Math. Soc.*, vol. 180, pp. 171–188, 1973.
[26] M. P. do Carmo, *Differential Geometry of Curves and Surfaces*. Englewood Cliffs, NJ: Prentice-Hall, 1976.
[27] E. Sontag, “Control of systems without drift via generic loops,” *IEEE Trans. Automat. Contr.*, vol. 40, no. 7, pp. 1210–1219, 1995.
[28] H. Sussmann and Y. Chitour, “A continuation method for nonholonomic path-finding problems,” in *IMA Workshop on Robot.*, 1993.
[29] A. Bicchi, D. Prattichizzo, and S. S. Sastry, “Planning motions of rolling surfaces,” in *Proc. 34th IEEE Int. Conf. Dec. Contr.*, 1995, pp. 2812–2817.
[30] via Beirut, 2-4, Trieste (IT)A. A. Agrachev and Y. L. Sachkov, “An intrinsic approach to the control of rolling bodies,” ISAS-International School for Advanced Studies, Tech. Rep. S.I.S.S.A. 114/99/M, September 1999.
[31] A. Bicchi, A. Marigo, and D. Prattichizzo, “Dexterity through rolling: Manipulation of unknown objects,” in *Proc. Int. Conf. on Robot. Automat.*, 1998, pp. 1583–1568.
[32] M. Ceccarelli, A. Marigo, S. Piccinocchi, and A. Bicchi, “Planning motions of polyhedral parts by rolling,” Algorithmica, vol. 26, no. 4, 2000, to be published.
[33] H. Arai and S. Tachi, “Dynamic control of a manipulator with passive joints in an operational coordinate space,” in *Proc. IEEE Int. Conf. Robotics and Automation*, Sacramento, CA, 1991, pp. 1188–1195.

Alessia Marigo was born in Italy in 1969. She received the Laurea degree in mathematics from the University of Pisa in 1994 and the Ph.D. degree in robotics from the University of Genova in 1999.

From 1995 to 1999 she worked on nonholonomic control systems and on discrete systems with quantized control at the Centro “E.Piaggio” of the University of Pisa. Since 1999 she is at SISSA/ISAS (International School for Advanced Studies) in Trieste, Italy. Her current research interests involve geometric control theory and applications.

Antonio Bicchi (S’87-M’89-SM’99) received the Laurea degree (*cum laude*) from the University of Pisa in 1984, and the Ph.D. from the University of Bologna, in 1988. He has been a Post-Doctoral Scholar at the Massachusetts Institute of Technology, Artificial Intelligence Laboratory, in 1988–1990.

He currently is an Associate Professor of system theory and of robotics, with the Department of Electrical Systems and Automation, University of Pisa, and the Interdept. Research Center “E. Piaggio,” where he serves as Associate Director and leads the Robotics Group. His main research interests are in the field of dextrous manipulation, including force/torque and tactile sensing and sensory control; dynamics, kinematics and control of complex mechanical systems; and motion planning and control for nonholonomic systems.

He is a Senior Member of IEEE and an Associate Editor of the IEEE TRANSACTIONS ON ROBOTICS AND AUTOMATION